NASA TECHNICAL NOTE

NASA TN D-7199

NASA TN D-7199

AERODYNAMIC EFFECTS OF FIVE LIFT-FAN POD ARRANGEMENTS ON AN UNPOWERED V/STOL TRANSPORT MODEL

by James L. Thomas, Danny R. Hoad, and Delwin R. Croom

Langley Research Center
and
Langley Directorate, U.S. Army Air Mobility R&D Laboratory
Hampton, Va. 23365

NATIONAL AERONAUTICS AND SPACE ADMINISTRATION • WASHINGTON, D. C. • JUNE 1973

1. Report No.	2. Government Accession No.	3. Recipient's Catalog No.
NASA TN D-7199		

4. Title and Subtitle	5. Report Date
AERODYNAMIC EFFECTS OF FIVE LIFT-FAN POD ARRANGEMENTS ON AN UNPOWERED V/STOL TRANSPORT MODEL	June 1973
	6. Performing Organization Code
7. Author(s) James L. Thomas, Langley Research Center; Danny R. Hoad, Langley Directorate, U.S. Army Air Mobility R&D Laboratory; and Delwin R. Croom, Langley Research Center	8. Performing Organization Report No. L-8754
	10. Work Unit No. 760-62-01-02
9. Performing Organization Name and Address NASA Langley Research Center Hampton, Va. 23665	11. Contract or Grant No.
	13. Type of Report and Period Covered Technical Note
12. Sponsoring Agency Name and Address National Aeronautics and Space Administration Washington, D.C. 20546	14. Sponsoring Agency Code

15. Supplementary Notes

16. Abstract

An investigation was conducted in the Langley V/STOL tunnel to determine the effect of longitudinally oriented wing-mounted pods on the longitudinal and lateral aerodynamic characteristics in the cruise flight condition of a high-wing V/STOL transport model. Five pod arrangements were tested – three configurations with in-line pods at 20, 40, or 60 percent semispan and two split pod configurations with rear pods at 20 percent semispan and front pods at 40 or 60 percent semispan. In general, addition of the pods to the model decreased the stability, increased the lift-curve slope, and alleviated the abrupt stall of the basic model. The configuration with pods at 20 percent semispan had an abrupt instability at 10^{o} angle of attack. All the configurations had lateral stability at sideslip angles from 5^{o} to -5^{o}. Very little difference in results existed between the configurations with pods at 40 and 60 percent semispan. Of the split pod configurations, the configuration with front pods at 40 percent semispan offered the best trimmed lift and lift-induced drag characteristics at high angles of attack. The configuration with in-line pods at 40 or 60 percent semispan provided the best cruise characteristics of all the pod configurations.

17. Key Words (Suggested by Author(s))	18. Distribution Statement
VTOL Cruise aerodynamics Static stability Integral lift engine	Unclassified – Unlimited

19. Security Classif. (of this report)	20. Security Classif. (of this page)	21. No. of Pages	22. Price*
Unclassified	Unclassified	62	$3.00

*For sale by the National Technical Information Service, Springfield, Virginia 22151

AERODYNAMIC EFFECTS OF FIVE LIFT-FAN POD ARRANGEMENTS ON AN UNPOWERED V/STOL TRANSPORT MODEL

By James L. Thomas, Danny R. Hoad,*
and Delwin R. Croom
Langley Research Center

SUMMARY

An investigation was conducted in the Langley V/STOL tunnel to determine the effect of longitudinally oriented wing-mounted pods on the longitudinal and lateral aerodynamic characteristics in the cruise flight condition of a high-wing V/STOL transport model. Five pod arrangements were tested – three configurations with in-line pods at 20, 40, or 60 percent semispan and two split pod configurations with rear pods at 20 percent semispan and front pods at 40 or 60 percent semispan. In general, addition of the pods to the model decreased the stability, increased the lift-curve slope, and alleviated the abrupt stall of the basic model. The configuration with pods at 20 percent semispan had an abrupt instability at 10° angle of attack. All the configurations had lateral stability at sideslip angles from 5° to -5°. Very little difference in results existed between the configurations with pods at 40 and 60 percent semispan. Of the split pod configurations, the configuration with front pods at 40 percent semispan offered the best trimmed lift and lift-induced drag characteristics at high angles of attack. The configuration with in-line pods at 40 or 60 percent semispan provided the best cruise characteristics of all the pod configurations.

INTRODUCTION

Research is being conducted by industry and NASA toward the development of a near-term VTOL aircraft to be used in short-haul transport applications. Considerable interest has arisen in the use of high-bypass-ratio integral fan engines to supply powered lift because of the high thrust-to-weight ratios and low noise levels attainable. In design concepts, these lift-fan engines provide direct lift during take-off and vectored lift and thrust during the transition to wing-supported flight. Larger jet engines provide thrust during the transition and cruising region of flight, where less restrictive noise considerations apply.

Recent designs have utilized the concept of longitudinally oriented pods mounted on the wing to encase the lift-fan engines (refs. 1 to 3). While the take-off and transition

---

*Langley Directorate, U.S. Army Air Mobility R&D Laboratory.

areas of flight for several pod configurations have been investigated (refs. 4 to 7), little attention has been directed toward the cruise region of flight, that in which the lift-fan pods are sealed and inoperative and only the cruise engines provide thrust.

The purpose of this investigation was to determine the effect of the wing-mounted pods on the longitudinal and lateral aerodynamic characteristics for the cruising flight condition. Five different lift-fan pod configurations were selected from current designs and experimental investigations. The static longitudinal and lateral aerodynamic characteristics for each unpowered configuration and the clean (no-pod) model are presented herein. Comparisons and analyses of the pod configurations are also made in order to determine a pod configuration that has the least adverse effects in cruise, particularly drag penalties introduced by the addition of the pods.

SYMBOLS

All the longitudinal forces and moments presented herein are referenced to the stability-axis system and all lateral forces and moments are referenced to the body-axis system. The data are referred to a moment center located in the plane of symmetry, vertically at the average center line of the lift-fan pods and, unless otherwise stated, longitudinally at the quarter-chord point of the mean aerodynamic chord of the wing.

Measurements and calculations were made in U.S. Customary Units. They are presented herein in the International System of Units (SI) with the equivalent values in U.S. Customary Units given parenthetically. Factors relating the two systems are given in reference 8.

b	wing span, meters (ft)
C_D	drag coefficient, D/qS
C_L	lift coefficient, L/qS
C_{L_α}	lift-curve slope, $\partial C_L/\partial\alpha$, per degree
C_l	rolling-moment coefficient, M_X/qSb
C_{l_β}	effective-dihedral parameter, $\Delta C_l/\Delta\beta$, from values of C_l for $\beta = 5^\circ$ and -5°, per degree
C_m	pitching-moment coefficient, $M_Y/qS\bar{c}$

$C_{m_{i_t}}$	horizontal-tail effectiveness parameter, $\partial C_m/\partial i_t$, per degree
C_n	yawing-moment coefficient, M_Z/qSb
C_{n_β}	directional-stability parameter, $\Delta C_n/\Delta\beta$, from values of C_n for $\beta = 5^o$ and -5^o, per degree
C_Y	side-force coefficient, F_Y/qS
C_{Y_β}	lateral-stability parameter, $\Delta C_Y/\Delta\beta$, from values of C_Y for $\beta = 5^o$ and -5^o, per degree
$\bar{c}$	mean aerodynamic chord, meters (ft)
D	drag force, newtons (lb)
F_Y	side force, newtons (lb)
H.T.	horizontal tail
i_t	horizontal-tail incidence angle (positive direction, trailing edge down), degrees
L	lift force, newtons (lb)
M_X	rolling moment, meter-newtons (ft-lb)
M_Y	pitching moment, meter-newtons (ft-lb)
M_Z	yawing moment, meter-newtons (ft-lb)
q	free-stream dynamic pressure, $\rho V^2/2$, newtons/meter^2 (lb/ft^2)
q_t	dynamic pressure at tail, newtons/meter^2 (lb/ft^2)
S	wing area, meters^2 (ft^2)
V	free-stream velocity, meters/second (ft/sec)

V.T. vertical tail

$\bar{x}$ longitudinal distance from leading edge of $\bar{c}$ to moment reference center, centimeters (in.)

α angle of attack, measured vertically between free stream and fuselage reference line (positive direction, nose up), degrees

β angle of sideslip, measured laterally between free stream and fuselage reference line (positive direction, nose left), degrees

ϵ downwash angle (positive direction, downflow), degrees

ρ air density, kilograms/meter^3 (slugs/ft^3)

Subscript:

trim at trim conditions

CONFIGURATIONS

Geometric characteristics of the basic high-wing transport model without the lift-fan pods attached (hereafter referred to as configuration 0) are shown in figure 1. Pertinent dimensions of the pods mounted on the wing are given in figures 2 and 3. For each configuration the pods were sized to accommodate a total of 10 lift-fan engines, each with a diameter-to-height ratio of 1.64. The pods were balanced longitudinally, assuming equal individual engine thrust, about the quarter-chord point of the mean aerodynamic chord. The in-line pod configurations, in which the pods were mounted at 20, 40, or 60 percent semispan (hereafter referred to as configurations 1, 2, and 3, respectively) are shown in figure 2. The split pod configurations, those in which the pods aft of the wing were mounted at 20 percent semispan and the pods forward of the wing were mounted at 40 or 60 percent semispan (hereafter referred to as configurations 4 and 5, respectively) are shown in figure 3. Longitudinal data were also obtained on configuration 6, which was the same as configuration 4 except that the trailing edge of the forward pod was modified to a more gradual fairing. (See fig. 3.) Photographs of two of the configurations mounted in the test section of the Langley V/STOL tunnel are shown in figure 4.

All the configurations had the same horizontal tail, for which the incidence could be varied from -15° to 15° in 5° increments. The horizontal and vertical tails and basic wing were removable to provide data for analysis.

TESTS AND CORRECTIONS

The investigation was conducted in the Langley V/STOL tunnel, which has a test section of 4.42 meters (14.50 ft) by 6.63 meters (21.75 ft). The model was sting supported on a six-component strain-gage balance which measured the forces and moments. Angle of attack was indicated by an electronic inclinometer mounted in the fuselage; angle of sideslip was measured by a mechanical counter on the strut which supported the sting.

All tests were run at a free-stream dynamic pressure of 2400 newtons/meter^2 (50.0 lb/ft^2), which corresponds to a velocity of 64 meters/second (210 ft/sec). The Reynolds number for the tests was approximately 1.35×10^6 based on the wing mean aerodynamic chord. Transition strips approximately 0.30 centimeter (0.12 in.) wide, of No. 60 abrasive grit, were placed 2.51 centimeters (0.99 in.) back of the leading edge of the airfoils, fuselage, and pods.

The basic longitudinal characteristics were obtained through an angle-of-attack range of -5° to 24°. Each configuration was tested at several tail incidence angles and with the horizontal tail off. Tuft studies were made at a low dynamic pressure for each configuration. Tests were made at sideslip angles of 5° and -5° over an angle-of-attack range of -5° to 24° to determine the static lateral-directional stability derivatives. For these lateral data each of the basic configurations was tested with the horizontal tail on and off, and with both vertical and horizontal tails off. A limited number of tests were made through an angle-of-sideslip range of -10° to 10° at angles of attack of 0°, 10°, and 20° to determine the linearity of the lateral stability characteristics.

Wind-tunnel boundary corrections (ref. 9), although slight, were applied to the data. Model-chamber pressure readings were taken, and corrections were applied to the drag data, although these corrections were also slight.

PRESENTATION OF RESULTS

The results of the wind-tunnel tests to determine the effects of the pods on the aerodynamic characteristics of the basic model in the cruise flight condition are presented in the following figures:

LONGITUDINAL AERODYNAMIC CHARACTERISTICS

The data in figure 5 indicate that the basic model (configuration 0) is stable and can be trimmed throughout the angle-of-attack range of the investigation. The variation of pitching moment with angle of attack is essentially linear up to the rather sharp stall at about 10° angle of attack (except for positive tail incidence, where effects of tail stall are evident). For a cruise lift coefficient of 0.40, the configuration can be trimmed at a horizontal-tail incidence of -3.3° with a static stability of $\partial C_m/\partial C_L = -0.44$. This high level of stability indicates that the horizontal tail provides too much stability for efficient flight with the assumed moment-center location at $0.25\bar{c}$. (A generally acceptable stability for cruise is $\partial C_m/\partial C_L = -0.05$.) Cruise trim penalties amount to an increase in drag coefficient of about 0.008 with a trimmed cruise-drag coefficient of 0.040. This cruise-drag coefficient includes the effect of a reduction in angle of attack required for cruise, which is less than $1/2^{\circ}$ because the uplift at the horizontal tail required for trim at $C_L = 0.40$ is small.

The static margin, the drag coefficient with tail off and lift coefficient of 0.40, and the lift-curve slope with 0° tail incidence have been computed from data shown in figures 5 to 11 and are presented in the following table:

Configuration	Static margin, fraction of $\bar{c}$	Drag coefficient, tail off $(C_L = 0.40)$	Lift-curve slope $(i_t = 0^{\circ})$
0	-0.44	0.034	0.090
1	-.05	.040	.098
2	-.27	.037	.094
3	-.29	.038	.096
4	-.26	.050	.097
5	-.27	.051	.099
6	-.26	.050	.099

As seen in the table, the static longitudinal stability of the basic model is decreased with the addition of the pods. The stability is most noticeably decreased for configuration 1. As shown in figure 6(b), this configuration has trim capability with positive stability up to an angle of attack of about 8°. The effectiveness of the tail diminishes at this point near the tail incidence for trim $(i_t \approx 0)$ and sooner at higher positive tail incidence.

Configurations 2 to 6 have static margins which are one-half to two-thirds that of the basic model, with trim capabilities throughout the angle-of-attack range of the investigation. The addition of the pods to the basic model alleviates its sharp stalling characteristics and increases C_{L_α} by as much as 10 percent for some of the configurations.

The untrimmed drag penalty associated with the addition of the pods was only about 0.005 for configurations 1, 2, and 3 but was about 0.015 for the split pod configurations because their pod frontal area was about twice that of configurations 1, 2, and 3.

Downwash at the Horizontal Tail

The variation of downwash angle at the horizontal tail with angle of attack is presented in figure 12 for each of the configurations tested. The incremental downwash angle resulting from the presence of the pods is generally small at all angles of attack except for configuration 1. Some slight decrease in downwash angle is seen at higher angles of attack when the pods are moved from 40 to 60 percent semispan. These data were taken from the tail-on and tail-off pitching-moment characteristics. Some of the data at high angles of attack have been extrapolated from plots of tail pitching moment as a function of tail incidence. Configurations 2, 3, and 5 have the most desirable downwash characteristics, which are similar to those of the basic model.

An attempt was made to determine the dynamic-pressure variation at the tail with angle of attack by comparing $C_{m_{i_t}}$ values for each configuration with $C_{m_{i_t}}$ values obtained in tests of the fuselage-tail combination. A band of data was generated which indicated values of q_t/q for this high horizontal tail between 0.91 and 0.97 for all the configurations and showed little variation with angle of attack.

The pitching-moment and lift-coefficient variations with angle of attack are presented in figure 13 for all the configurations with $i_t = -5^\circ$. The various stability levels are generally greater than that required for efficient flight.

Comparisons at Similar Stabilities

To be valid, comparisons of the trimmed lift and drag must be made at similar levels of stability; therefore, the stabilities of the various configurations were adjusted by transferring the moment reference center aft from the original location at $0.25\bar{c}$ to provide a static margin of $\partial C_m/\partial C_L = -0.05$. Comparisons of the configurations at a common level of stability $\left(\partial C_m/\partial C_L = -0.05\right)$ for untrimmed and trimmed conditions are presented in figures 14 to 18. Comparisons are made among configurations 0, 1, 2, and 3 with the tail off and at $i_t = 0^\circ$ in figure 14. With the horizontal tail at 0°, configuration 1 shows a large instability past wing stall at about 10° angle of attack. Values of tail-off pitching moment for configurations 2 and 3 differ little from those for configuration 0. Comparisons of tail-off with tail-on data indicate differences in stability at high angles of attack which can be attributed to increasing $\partial\epsilon/\partial\alpha$ at high angles (fig. 12) and tail stall effects.

The trimmed data in figure 16 indicate that small tail incidence settings can trim the configurations throughout the angle-of-attack range of the tests. The only penalties

in trimming the configurations are small drag increases because of the download at the tail required for trim. Maximum trimmed angle of attack for configuration 1 is about 16° because of tail stall, as shown in figure 6(b). Configuration 1 (pods at 20 percent semispan) offers the highest trimmed lift-curve slope and the lowest level of drag at the higher lift coefficient; but this configuration is very unstable past wing stall. Little difference in stability and performance is seen between configurations 2 and 3. Both have incremental drag coefficient increases from the basic configuration of about 0.005 at low angles of attack. All three configurations give much higher maximum lift coefficients than the basic model.

Figure 15 compares configurations 0, 4, 5, and 6 with the tail off and with $i_t = 0^{\circ}$. At angles of attack below stall there is little difference among configurations 4, 5, and 6 in untrimmed lift and drag. The modification to the trailing edge of the front pods of configuration 4 (resulting in configuration 6) provides a modest improvement in lift and lift-induced drag at angles of attack above wing stall. This fairing modification offers encouragement that modest improvements can be made in the lift and drag for all the configurations. However, it is believed that the relative differences in the aerodynamic characteristics among the pod configurations would not be affected by these modifications in fairings.

Tuft studies during the tests indicated several areas where improved flow might be obtained. The flow over the leading edges of all the pods was attached except on configuration 1, where the leading edges of the pods showed unsteady flow characteristics similar to those of the pod-wing intersections. There was separation at the trailing edges of all the pods, as expected. This separation was greatest for the split pod configurations.

The trimmed lift-drag polars in figure 17 for configurations 0, 4, 5, and 6 indicate that only small tail incidence settings are required to trim the split pod configurations throughout the angle-of-attack range of the tests. Configuration 5 requires more negative tail incidence than configuration 4 for trim at high angles of attack. Consequently, lift and lift-induced-drag characteristics for the former are less desirable past wing stall. The drag-coefficient increases due to the pods are about 0.015 for configurations 4, 5, and 6 at low angles of attack.

The trimmed lift and drag results for the best of the split pod configurations (configuration 6) and the best of the in-line pod configurations (configuration 2) are compared in figure 18. The split pod configuration has a higher minimum drag coefficient, about 0.041 as compared with about 0.033 for the in-line pod configuration. Lift and drag differences at high angles of attack are slight. Configuration 2 shows the best longitudinal cruise characteristics, largely because the drag is lower than that of the other pod configurations.

LATERAL-DIRECTIONAL STABILITY CHARACTERISTICS

The effects of the empennage on the variation of the static lateral-directional stability derivatives throughout an angle-of-attack range of -5° to 24° are presented in figure 19 for configurations 0 to 5. These derivatives were computed from data obtained at sideslip angles of 5° and -5°. Presented in figure 20 is the variation of the lateral aerodynamic characteristics with angle of sideslip at angles of attack of approximately 0°, 10°, and 20°. The slopes from these data show good overall agreement with the derivatives presented in figure 19 for sideslip angles up to at least 6°. In most cases, however, the variation of lateral components at high sideslip angles (8° to 10°) is appreciably less than that indicated by the derivatives at low sideslip angles.

All the model configurations investigated with the vertical tail on have positive static directional stability over the angle-of-attack range of the tests (fig. 19). Addition of the horizontal tail to the vertical tail provides the normal end-plate effect and increases the vertical-tail contribution to the lateral-stability derivatives.

At high angles of attack, there is some decrease in directional stability for the pod configurations. The largest effect of the pods on the lateral-stability derivatives is on the effective-dihedral parameter C_{l_β}. When compared with the basic configuration, placing the pods at 20 percent semispan generally increased the effective dihedral $\left(-C_{l_\beta}\right)$, and placement of the pods farther outboard reduced the effective dihedral at high angles of attack.

Since comparisons and evaluations of the longitudinal aerodynamic characteristics of the pods were made with a transferred moment reference center, the static lateral-directional derivatives with the transferred moment references were examined. Figure 21 presents only the directional-stability parameters C_{n_β} for configurations 0 to 5 since the transfers of the moment centers were only longitudinal.

In general, transferring the moment center to provide acceptable longitudinal stability reduced the directional stability of the configurations. All the configurations with the vertical tail, however, had positive directional stability.

SUMMARY OF RESULTS

An investigation was conducted in the Langley V/STOL tunnel to determine the effect of longitudinally oriented wing-mounted pods on the longitudinal and lateral aerodynamic characteristics in the cruise-flight condition of a high-wing V/STOL transport model. Five pod arrangements were tested – three configurations with in-line pods at 20, 40, or 60 percent semispan and two split pod configurations with rear pods at 20 percent semispan and front pods at 40 or 60 percent semispan. The results from this investigation are summarized as follows:

1. In general, addition of the pods to the model decreases the stability, increases the trimmed lift-curve slope before stall, and alleviates the abrupt stall of the basic model. At low angles of attack, the drag coefficient for the basic configuration is 0.030. The various pod configurations raise this basic value to the 0.035 to 0.045 range.

2. The model configuration with pods at 20 percent semispan has an abrupt instability for angles of attack above 10° and can be trimmed only to an angle of attack of 16° because of tail stall effects.

3. Little difference is noted between results with the pods at 40 percent semispan and at 60 percent semispan. Both model configurations have drag-coefficient increases due to pods of about 0.005 at low angles of attack, positive lateral stability through a sideslip range from 5° to -5°, and longitudinal trim capability throughout the angle-of-attack range of the tests (-5° to 24°).

4. The split pod configurations have drag coefficient increases due to the pods of about 0.015 at low angles of attack. They have positive lateral stability and can be trimmed through the angle-of-attack range of the tests. Of the split pod configurations, the configuration with front pods at 40 percent semispan offers better trimmed lift and lift-induced-drag characteristics at high angles of attack.

5. For the split pod configuration with front pods at 40 percent semispan, a modified fairing of the trailing edge of the front pods provides a modest improvement in lift and lift-induced drag past wing stall. Tuft studies during the tests indicated several areas on other pod configurations where similar improvements might be expected.

6. The configuration with in-line pods at 40 or 60 percent semispan provides the best cruise characteristics of all the pod configurations.

Langley Research Center,
National Aeronautics and Space Administration,
Hampton, Va., April 3, 1973.

REFERENCES

1. Carline, A. J. K.; and Velton, E. J.: Design Problems of a Commercial Jet Lift VTOL Transport. Proceedings of V/STOL Technology and Planning Conference, AF Flight Dynamics Lab., U.S. Air Force, Sept. 1969.

2. Holzhauser, Curt A.; Morello, Samuel A.; Innis, Robert C.; and Patton, James M., Jr.: A Flight Evaluation of a VTOL Jet Transport Under Visual and Simulated Instrument Conditions. NASA TN D-6754, 1972.

3. Szlenkier, T. K.: Latest Civilian V/STOL Aircraft Projects of Hawker Siddeley Aviation. NASA TT F-14,629, 1972.

4. Newsom, William A., Jr.: Wind-Tunnel Investigation of a V/STOL Transport Model With Four Pod-Mounted Lift Fans. NASA TN D-5942, 1970.

5. Newsom, William A., Jr.; and Moore, Frederick L.: Wind-Tunnel Investigation of a V/STOL Transport Model With Six Wing-Mounted Lift Fans. NASA TN D-5695, 1970.

6. Dickinson, Stanley O.; Hall, Leo P.; and Hodder, Brent K.: Aerodynamic Characteristics of a Large-Scale V/STOL Transport Model With Tandem Lift Fans Mounted at Mid-Semispan of the Wing. NASA TN D-6234, 1971.

7. Kirk, Jerry V.; Hall, Leo P.; and Hodder, Brent K.: Aerodynamics of Lift Fan V/STOL Aircraft. NASA TM X-62,086, 1971.

8. Mechtly, E. A.: The International System of Units – Physical Constants and Conversion Factors (Revised). NASA SP-7012, 1969.

9. Pope, Alan; and Harper, John J.: Low-Speed Wind Tunnel Testing. John Wiley & Sons, Inc., c.1966.

Wing	
Airfoil section; NACA 65A010 (tip), NACA 65A015(root)	
Area, m2 (ft2)	483 (5.202)
Mean aerodynamic chord, m (ft)	.268 (.879)
Span, m (ft)	1.902 (6.240)
Aspect ratio	7.50
Horizontal tail	
Airfoil section; 11% thick supercritical	
Area, m2 (ft2)	.144(1.551)
Mean aerodynamic chord, m(ft)	.213 (.699)
Span, m(ft)	.796(2.613)
Aspect ratio	4.40
Vertical tail	
Airfoil section; 11% thick supercritical	
Area, m2 (ft2)	.138 (1488)
Mean aerodynamic chord, m(ft)	.294 (.964)
Span, m(ft)	.488(1.600)

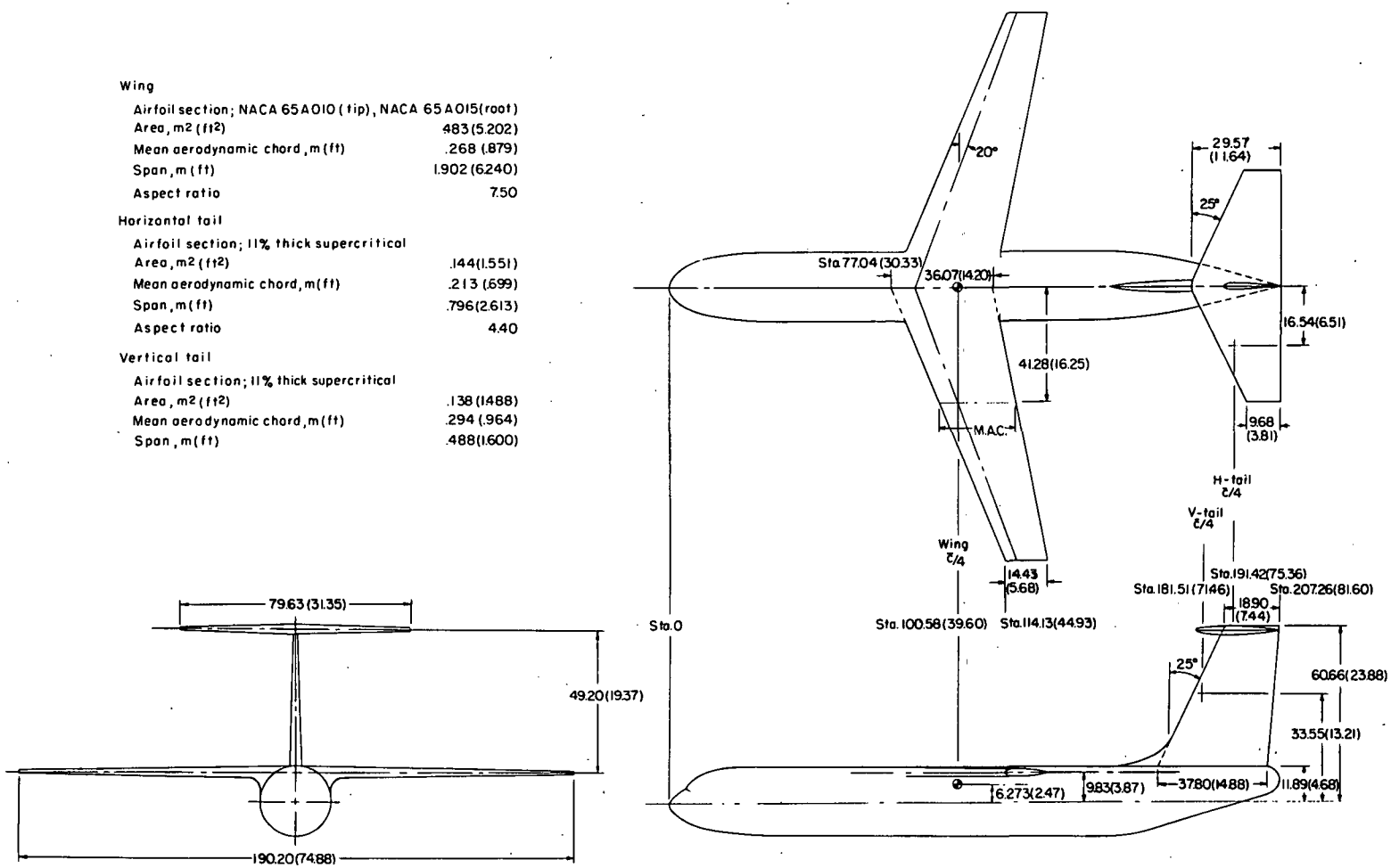

Figure 1.- Dimensions and characteristics of the basic model (configuration 0). Dimensions are in centimeters (inches).

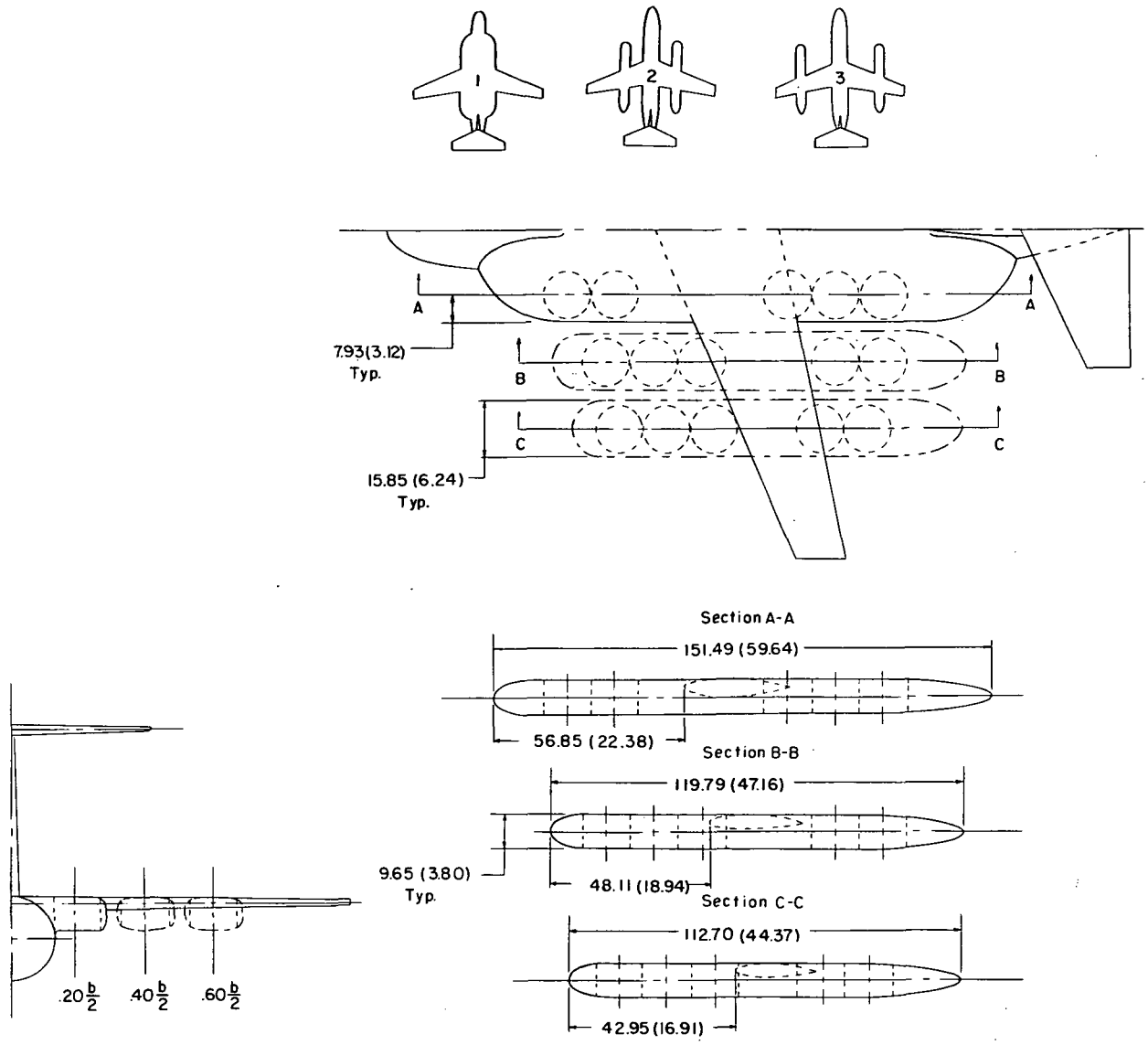

Figure 2.- Configurations with pods at 20, 40, or 60 percent semispan (configurations 1, 2, and 3). Dimensions are in centimeters (inches).

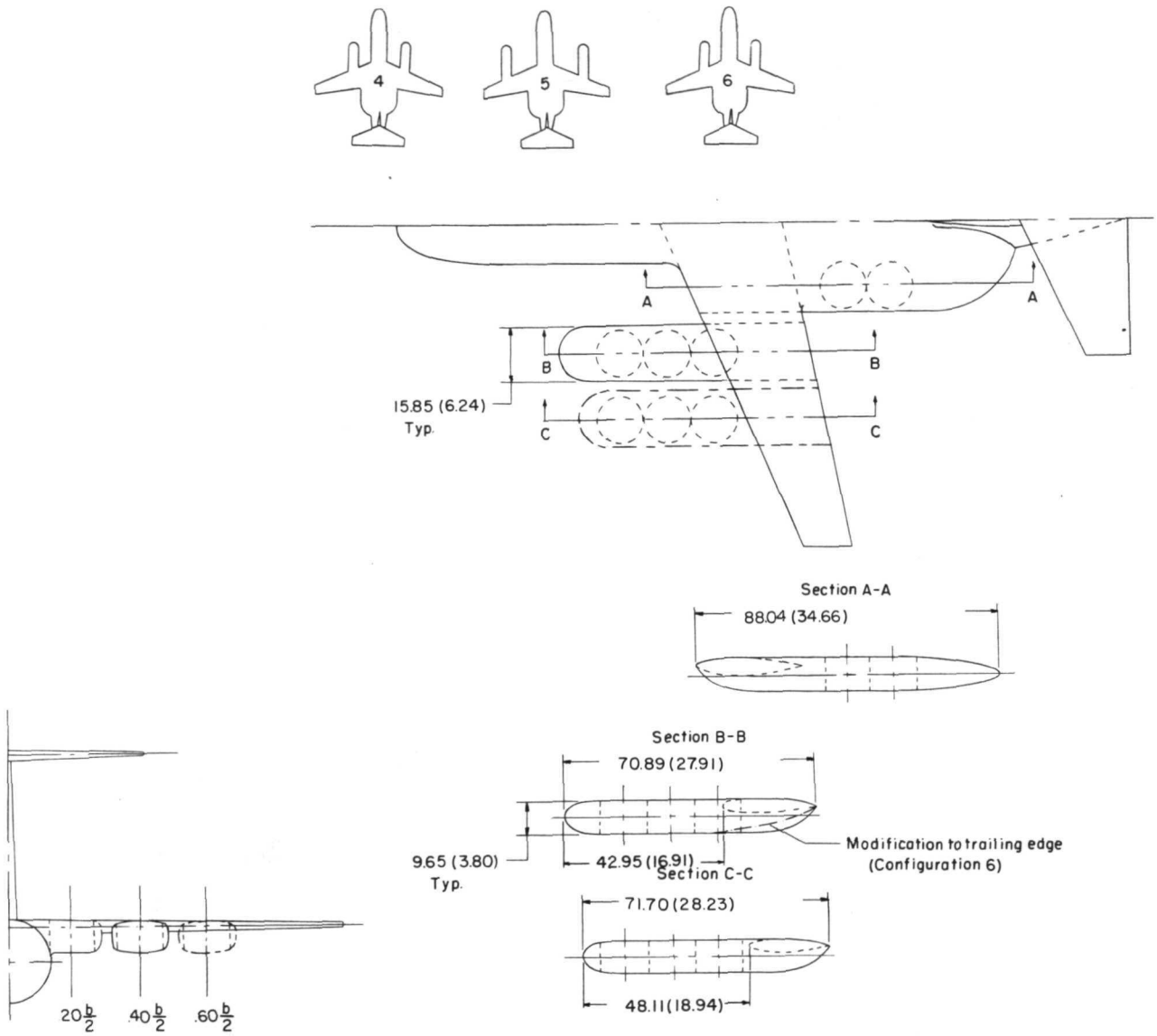

Figure 3.- Split pod configurations with rear pods at 20 percent semispan and front pods at 40 percent semispan (configurations 4 and 6) or 60 percent semispan (configuration 5). Dimensions are in centimeters (inches).

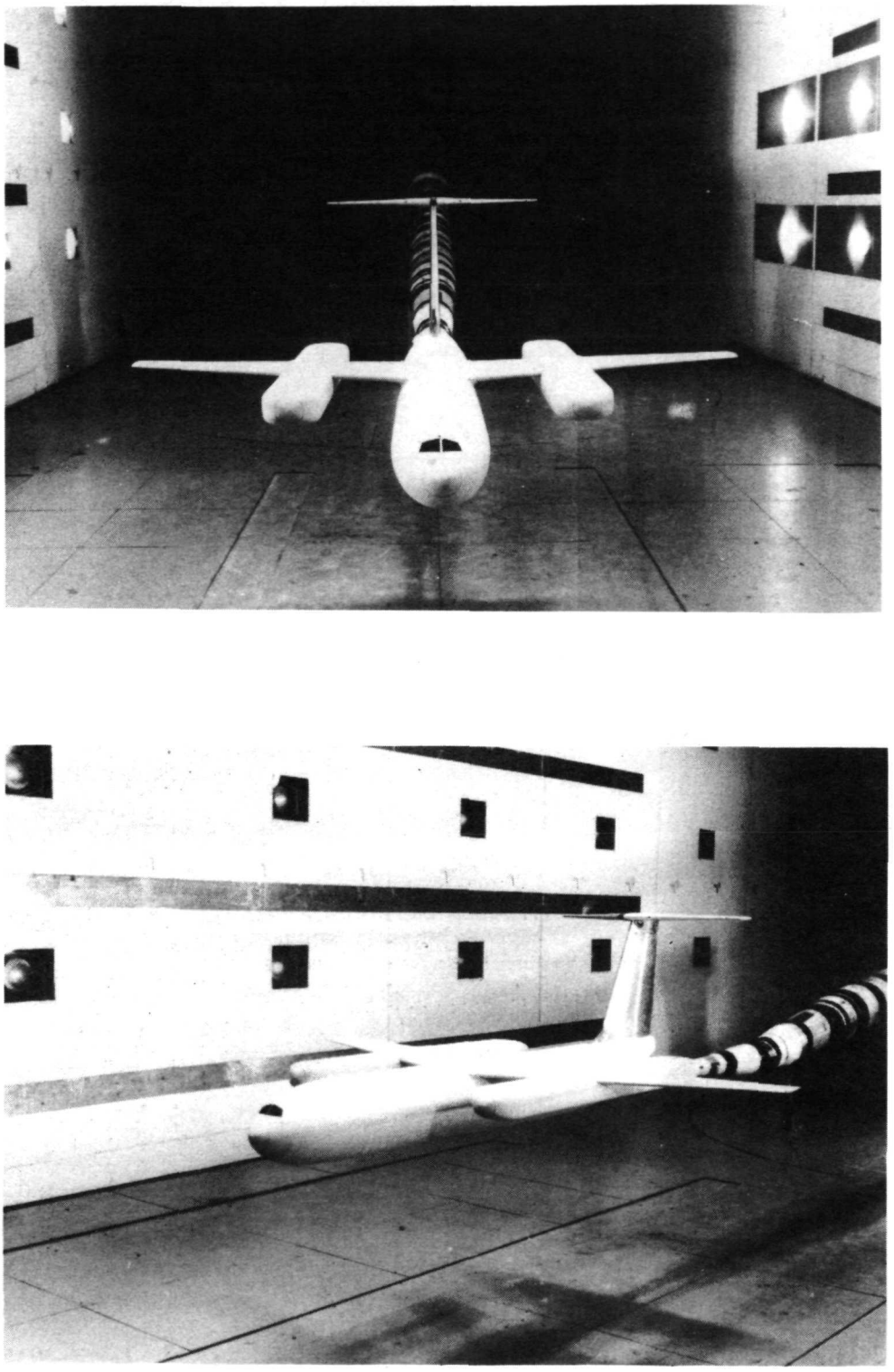

L-73-3018

(a) Configuration 2.

Figure 4.- Models in Langley V/STOL tunnel.

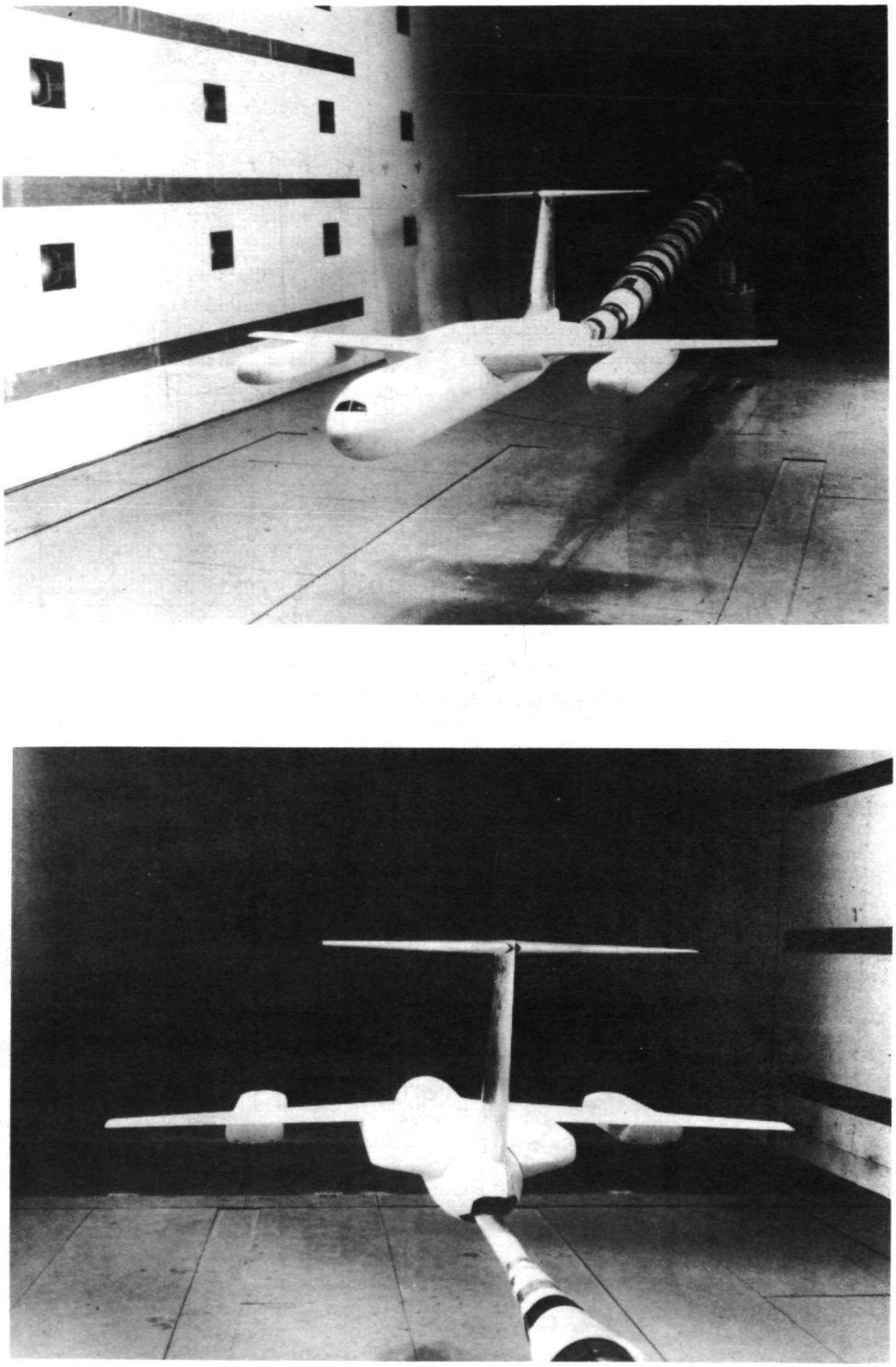

L-73-3019

(b) Configuration 5.

Figure 4.- Concluded.

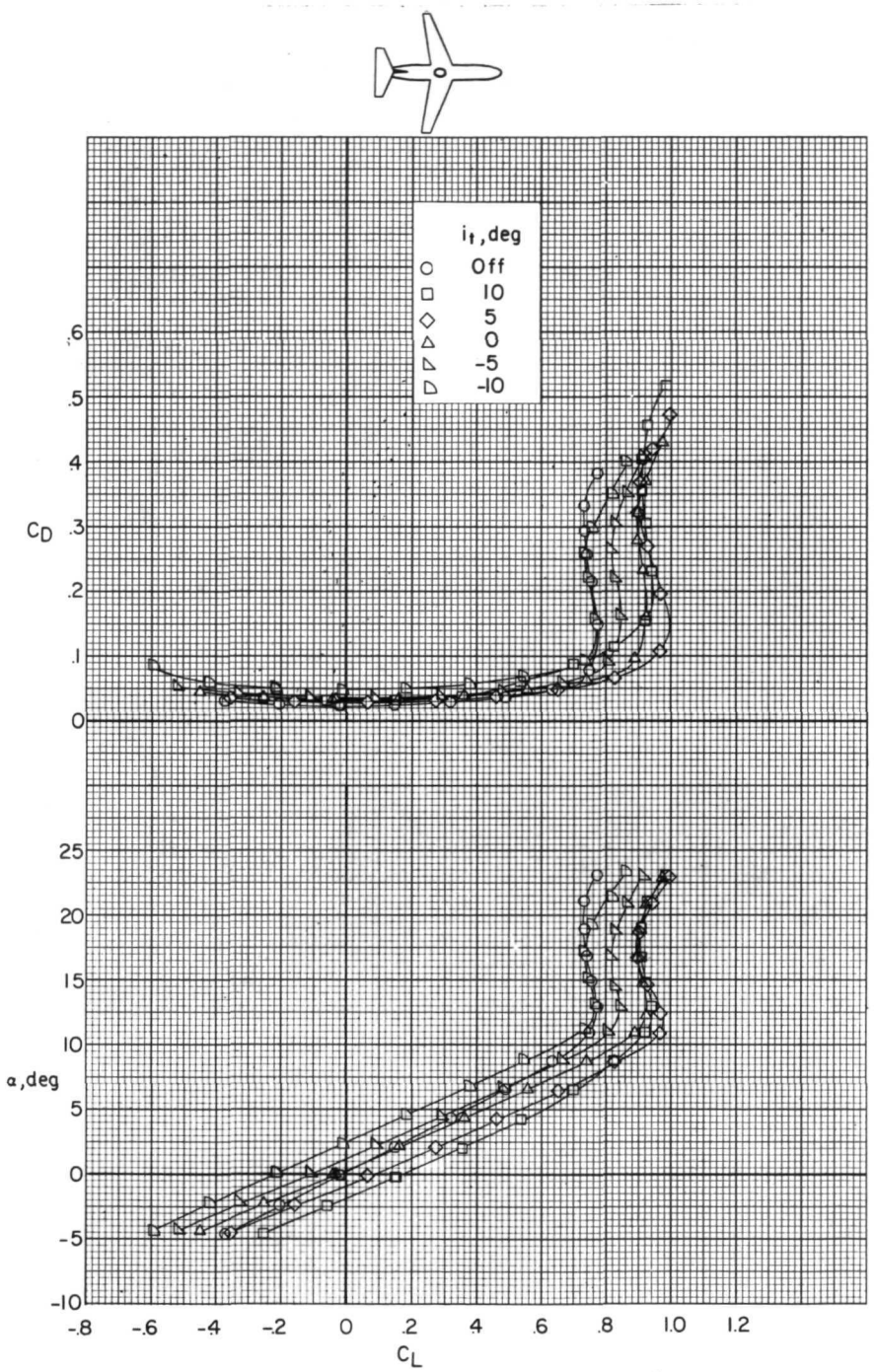

(a) Lift and drag coefficients.

Figure 5.- Effect of horizontal-tail incidence on longitudinal aerodynamic characteristics of configuration 0.

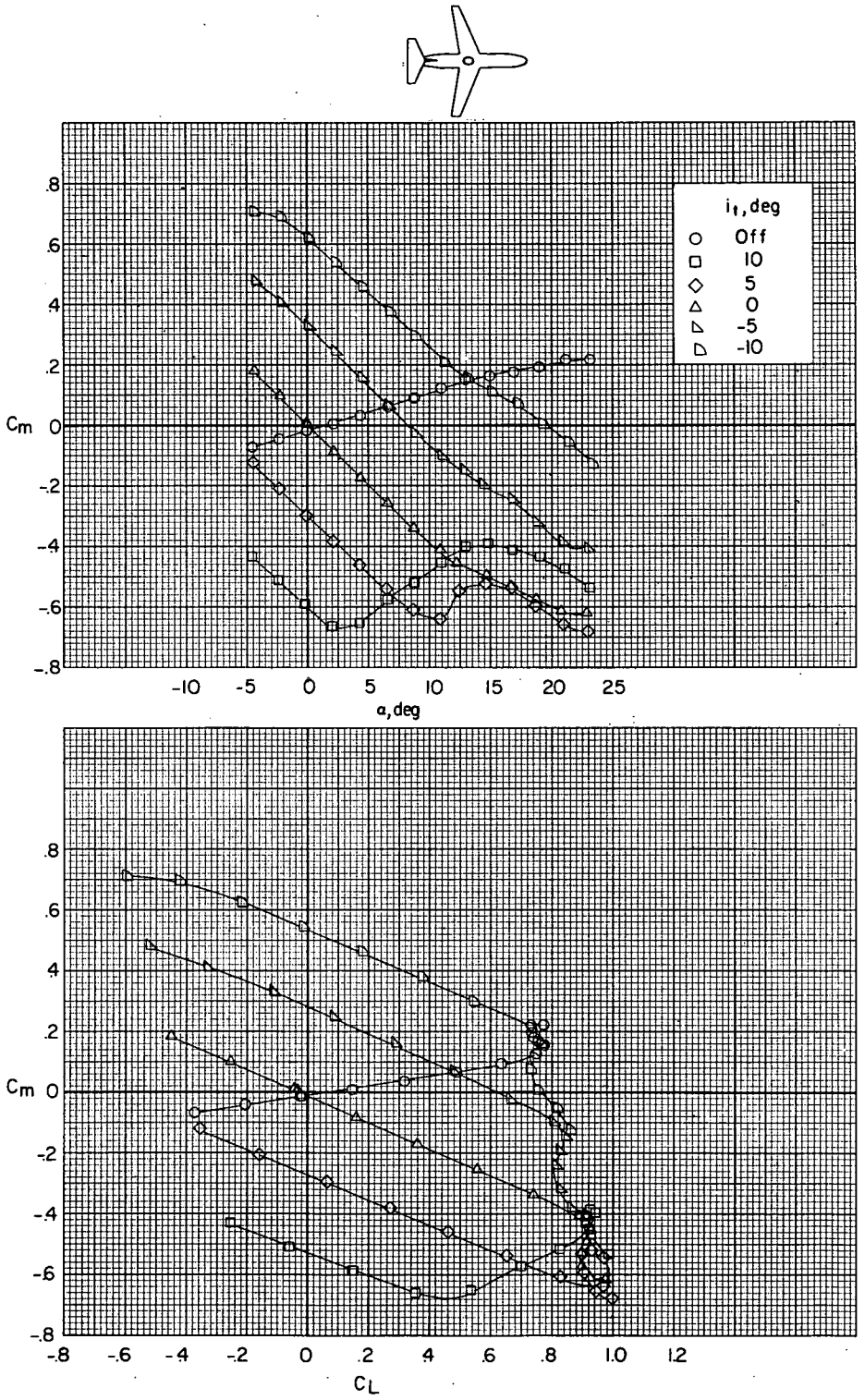

(b) Pitching-moment coefficient.

Figure 5.- Concluded.

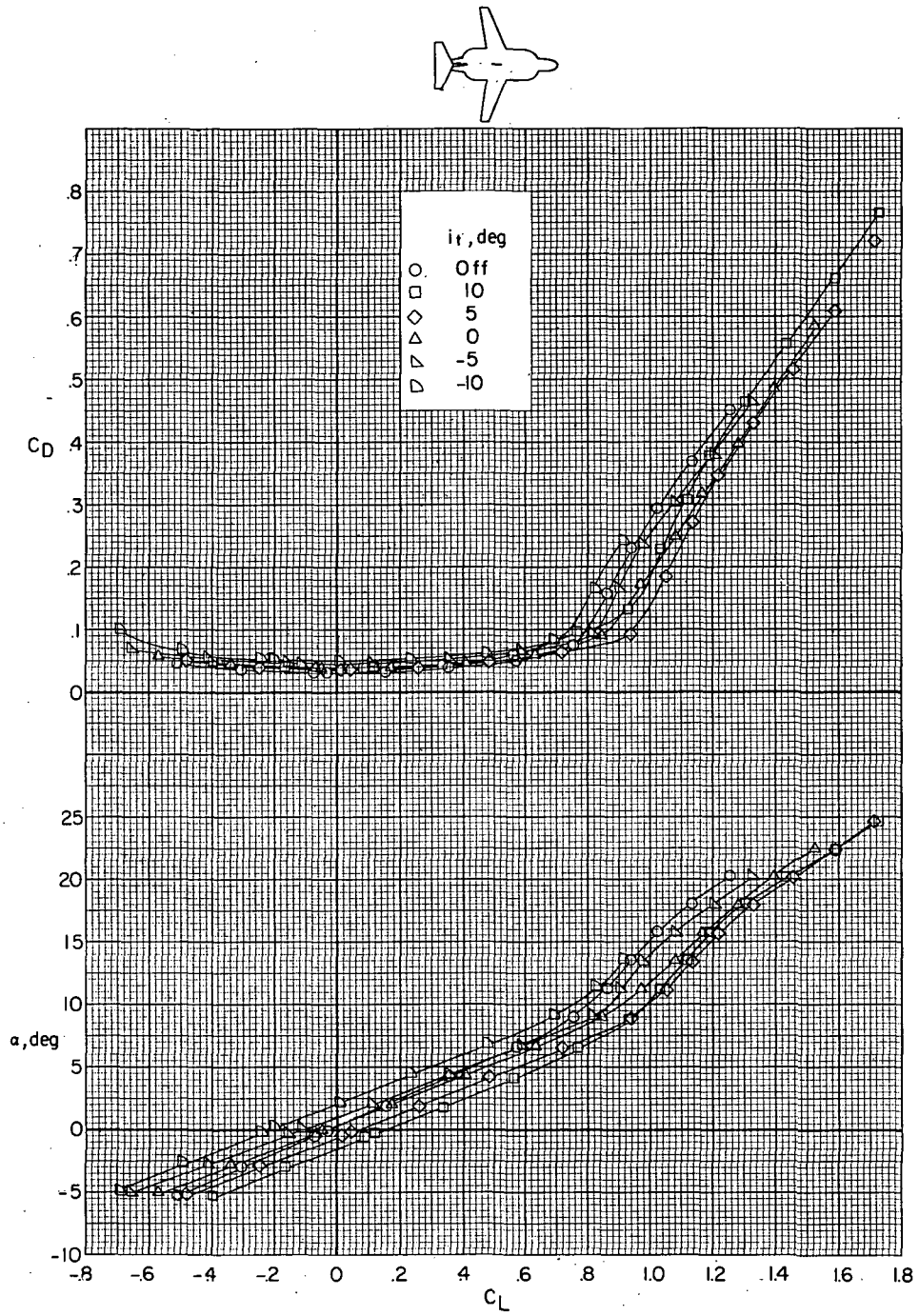

(a) Lift and drag coefficients.

Figure 6.- Effect of horizontal-tail incidence on longitudinal aerodynamic characteristics of configuration 1.

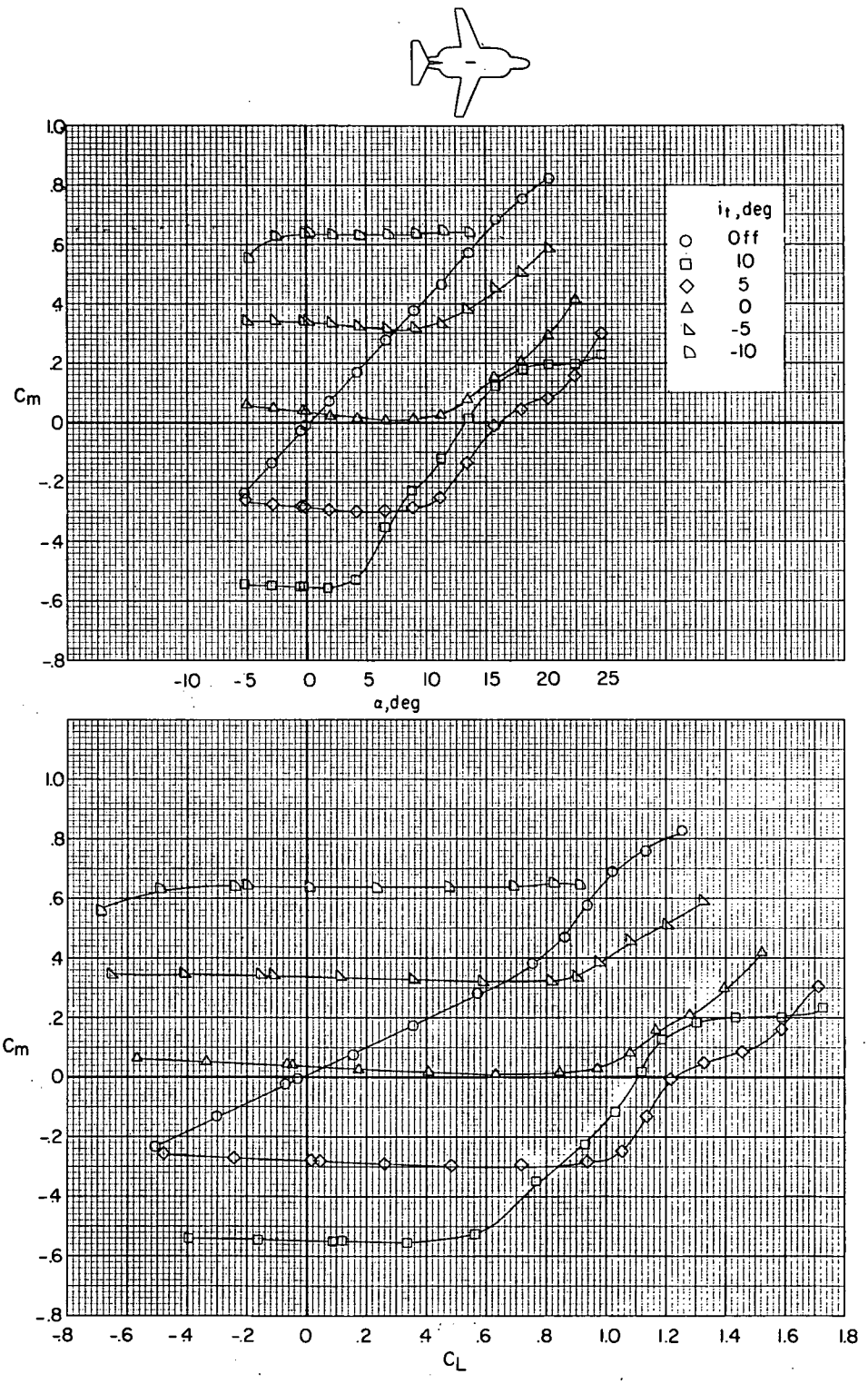

(b) Pitching-moment coefficient.

Figure 6.- Concluded.

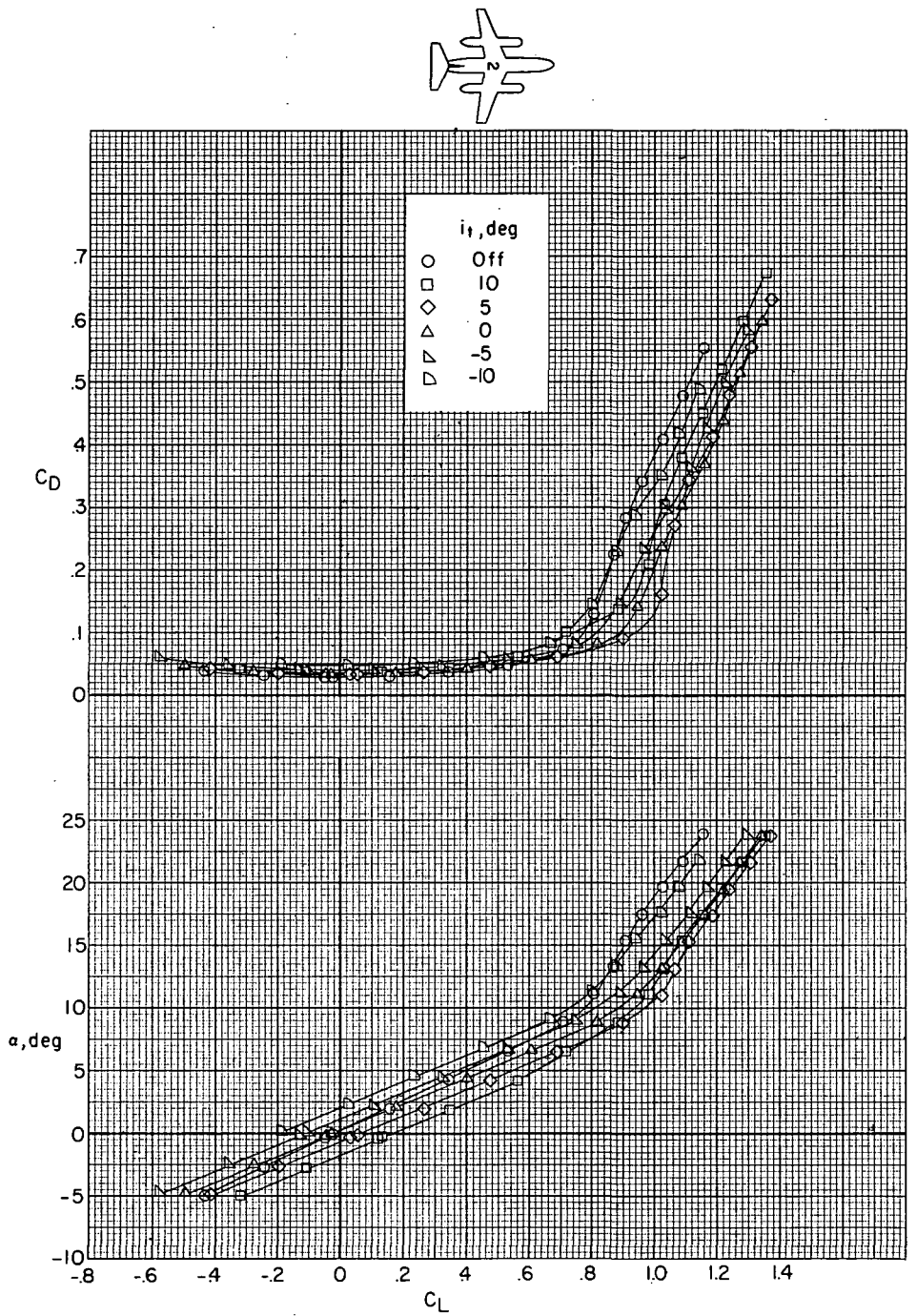

(a) Lift and drag coefficients.

Figure 7.- Effect of horizontal-tail incidence on longitudinal aerodynamic characteristics of configuration 2.

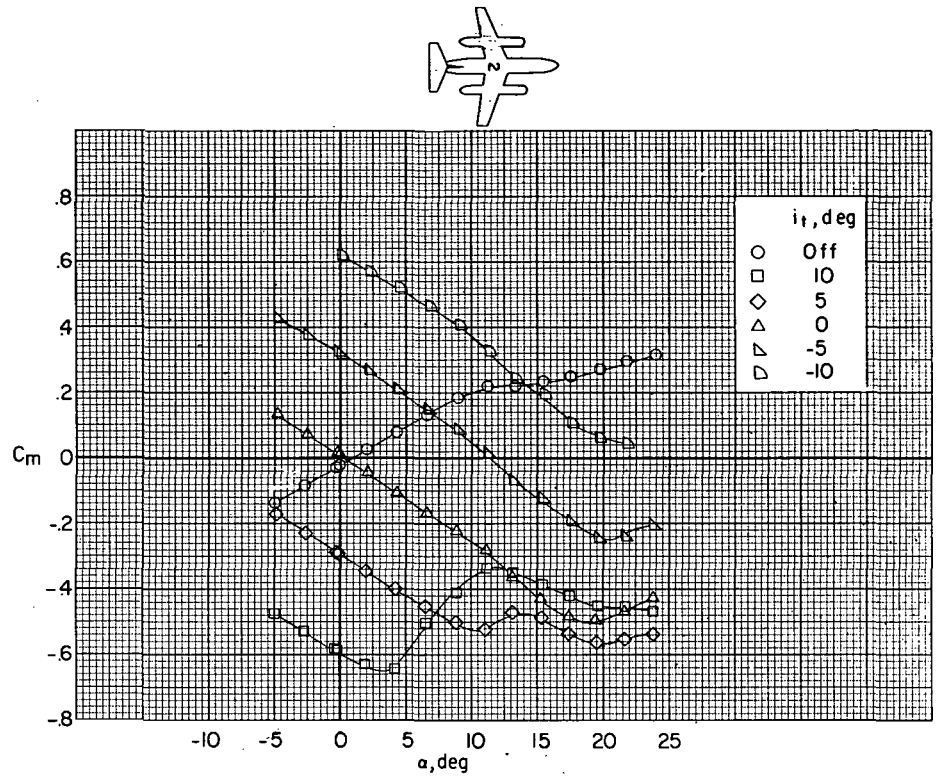

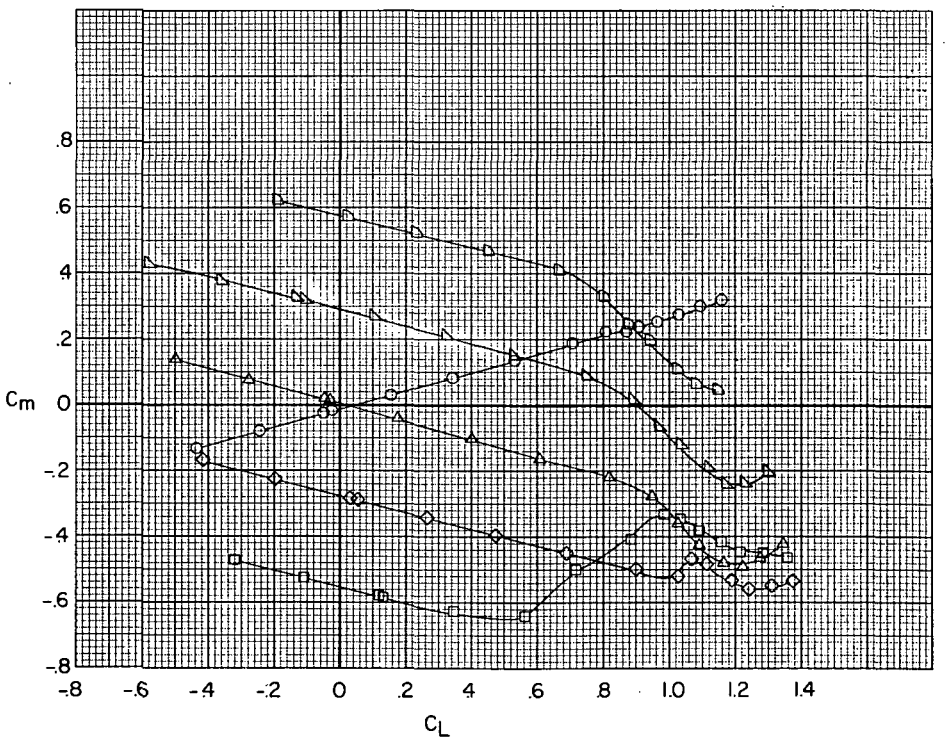

(b) Pitching-moment coefficient.

Figure 7.- Concluded.

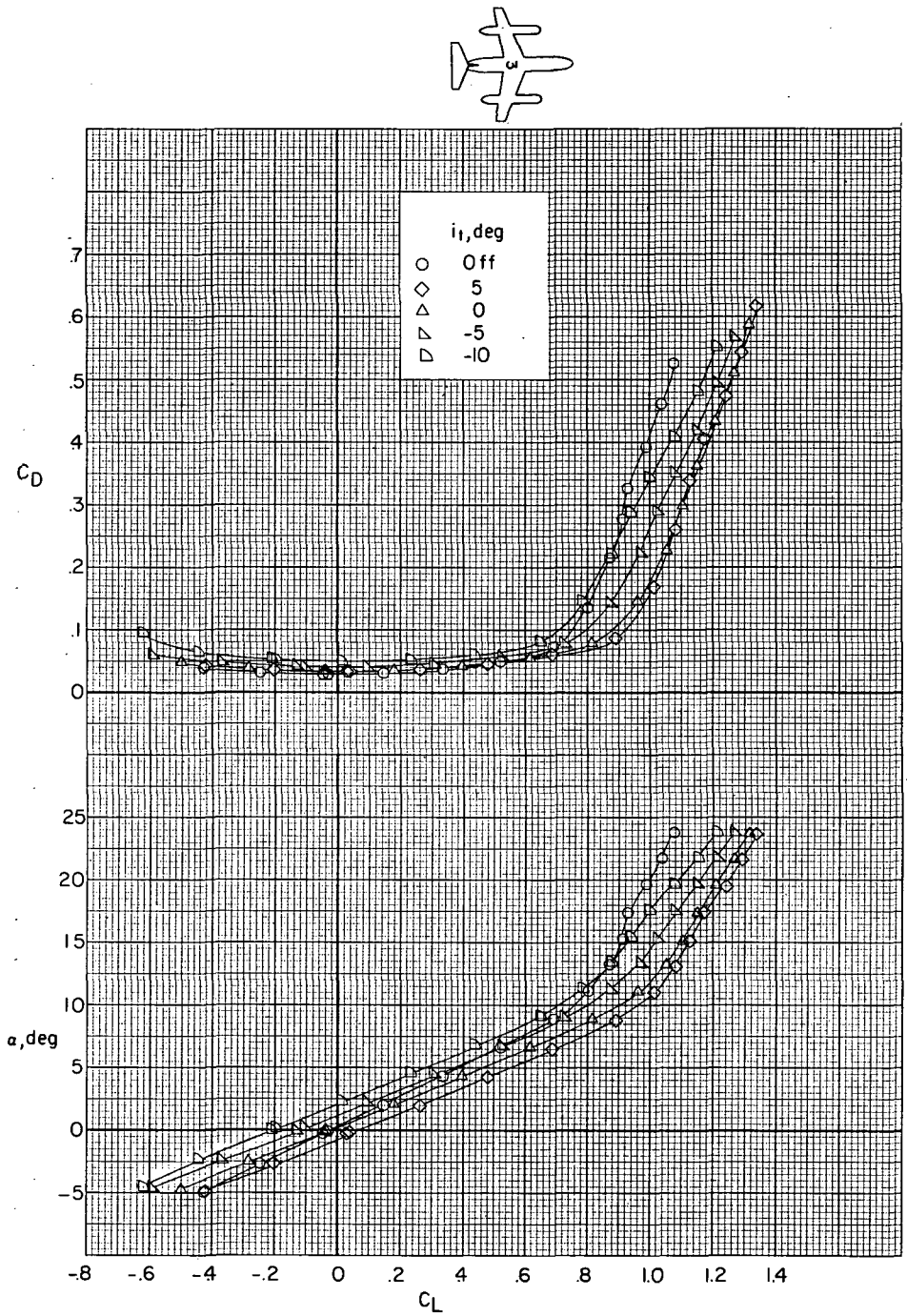

(a) Lift and drag coefficients.

Figure 8.- Effect of horizontal-tail incidence on longitudinal aerodynamic characteristics of configuration 3.

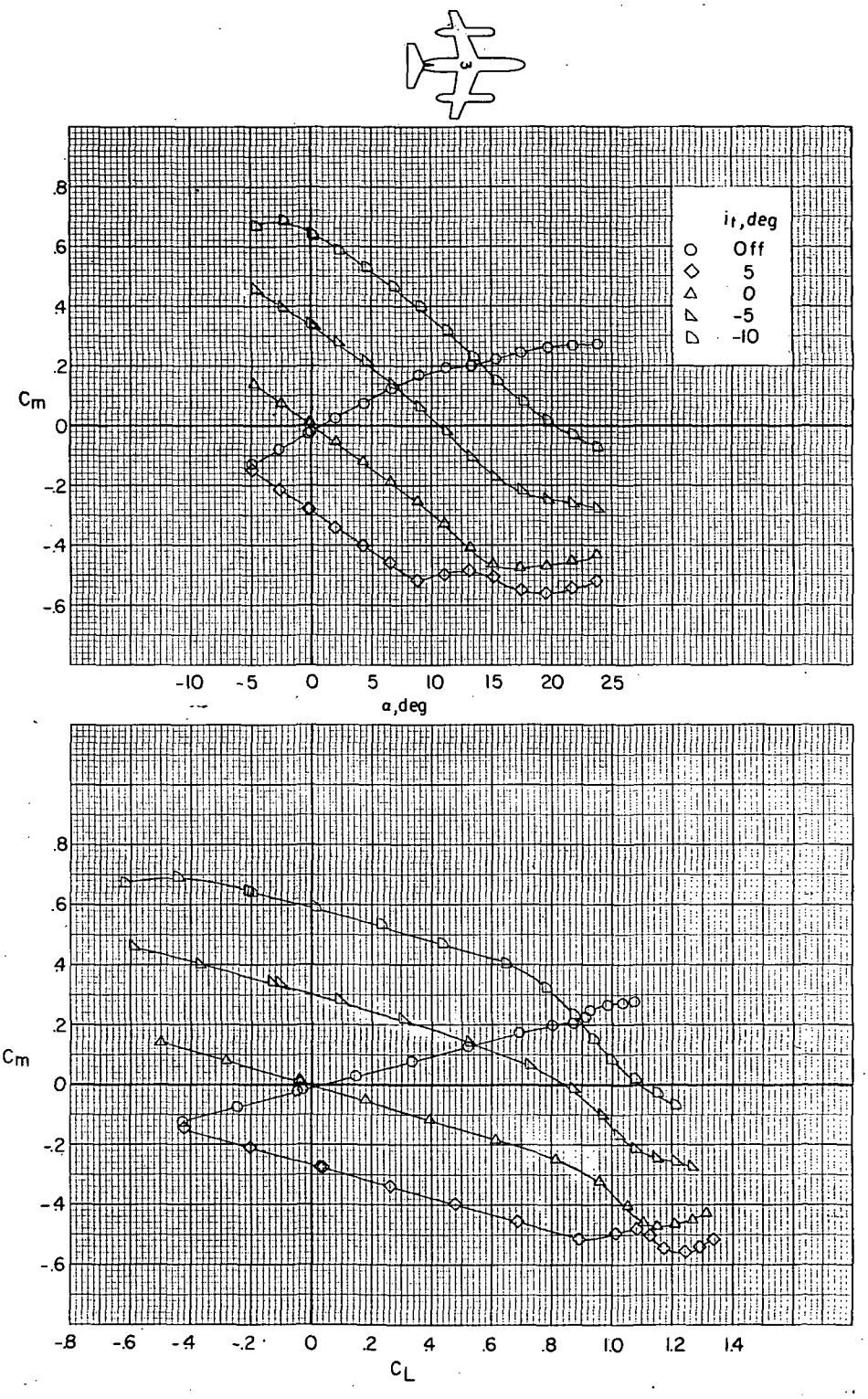

(b) Pitching-moment coefficient.

Figure 8.- Concluded.

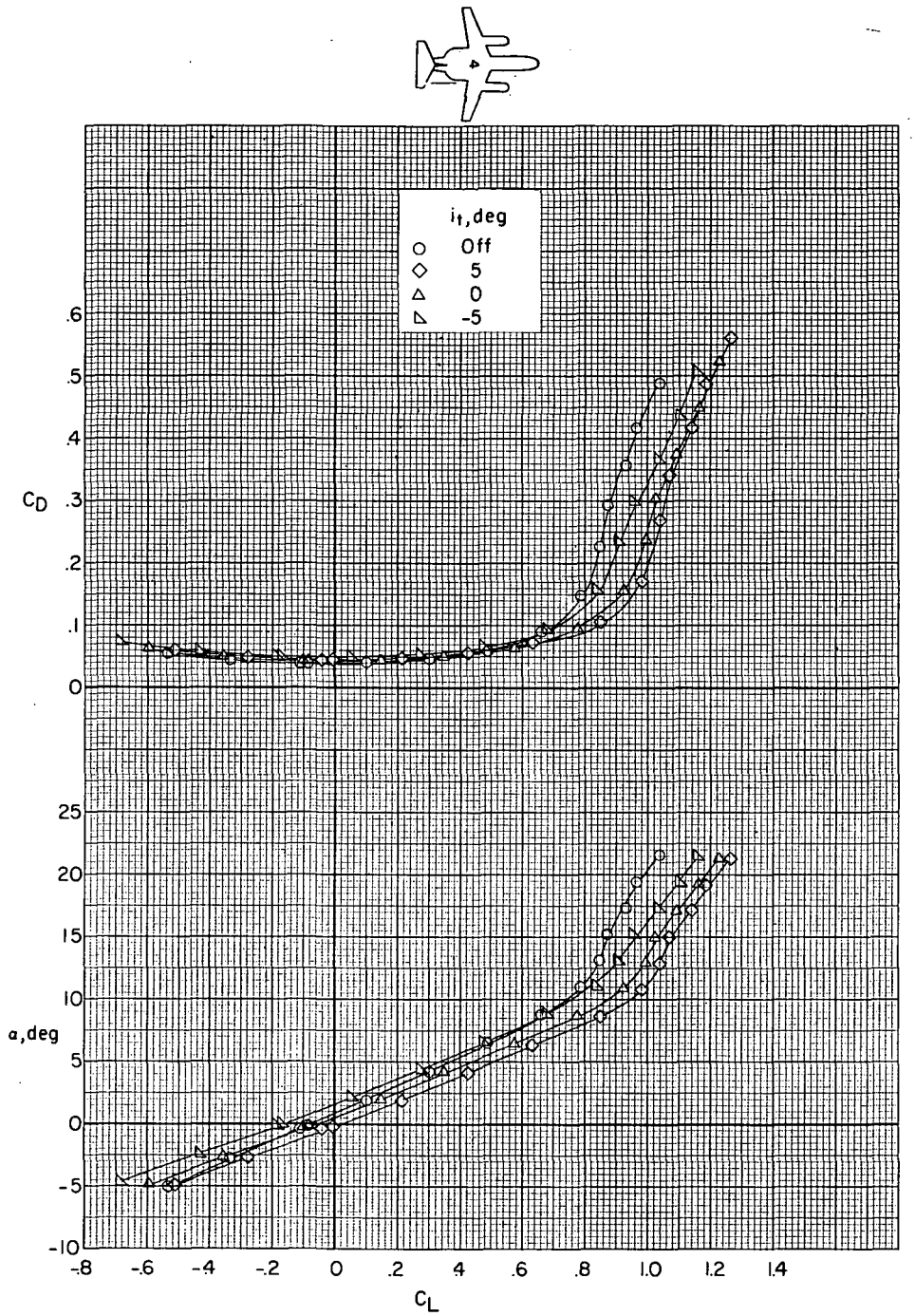

(a) Lift and drag coefficients.

Figure 9.- Effect of horizontal-tail incidence on longitudinal aerodynamic characteristics of configuration 4.

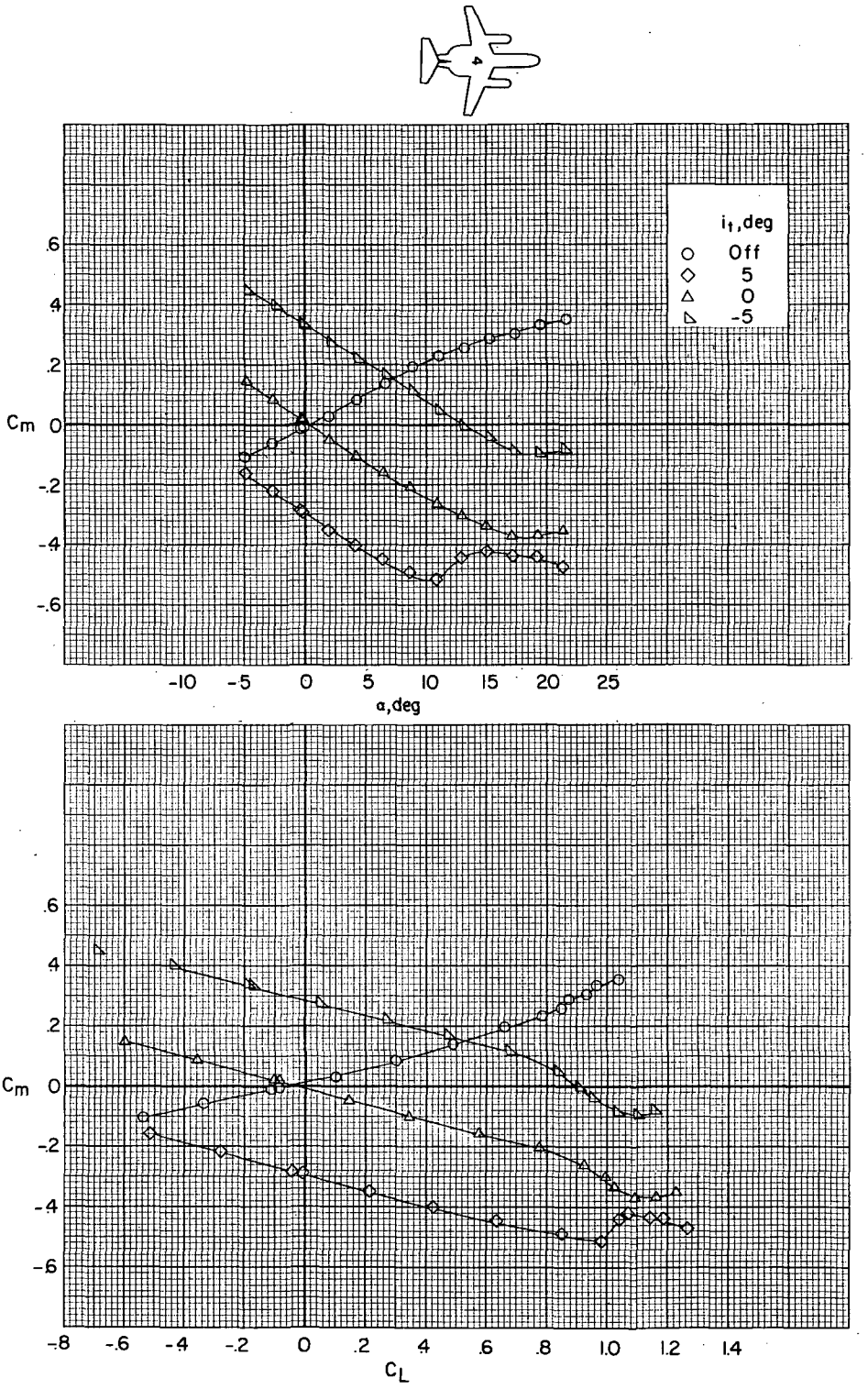

(b) Pitching-moment coefficient.

Figure 9.- Concluded.

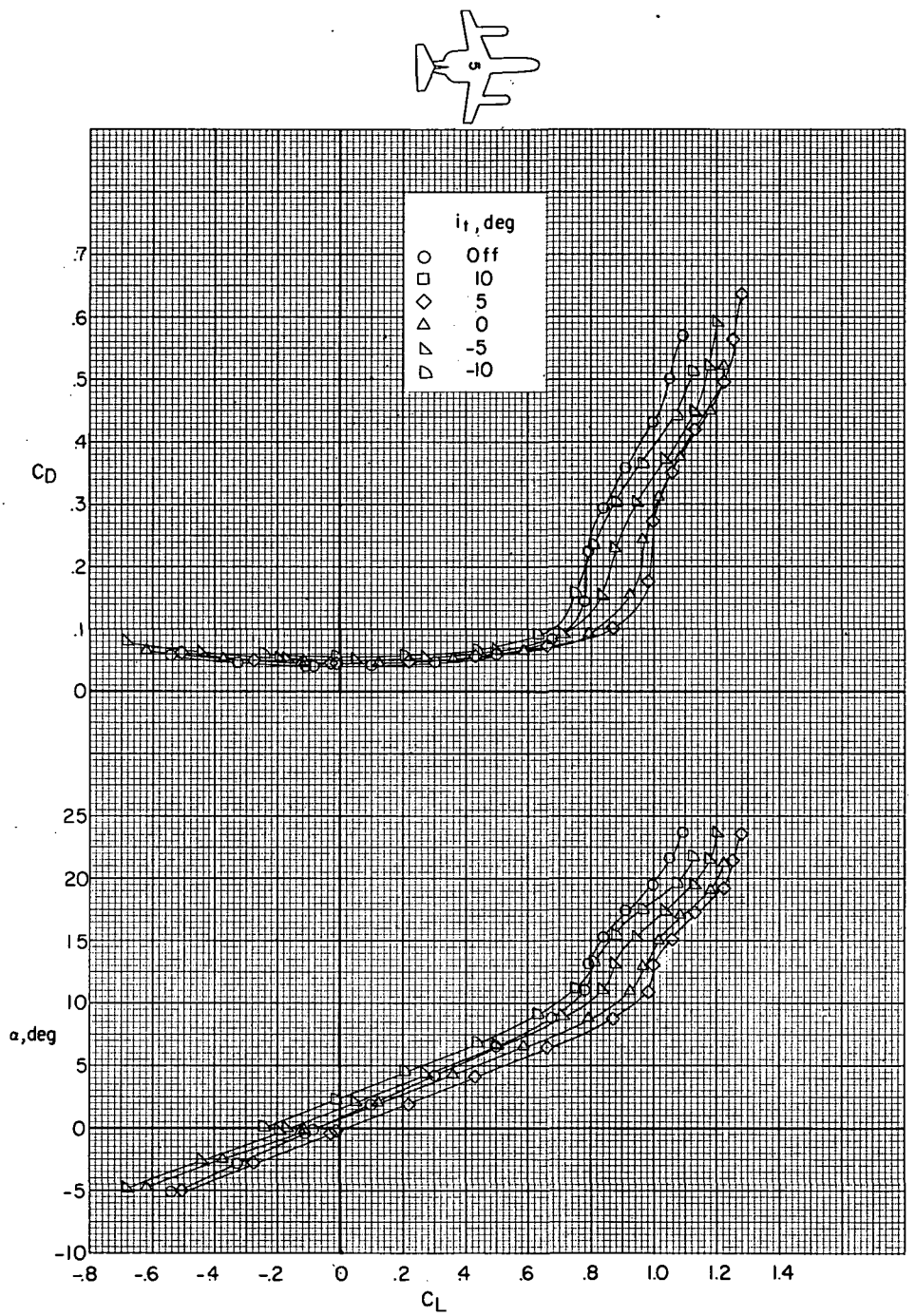

(a) Lift and drag coefficients.

Figure 10.- Effect of horizontal-tail incidence on longitudinal aerodynamic characteristics of configuration 5.

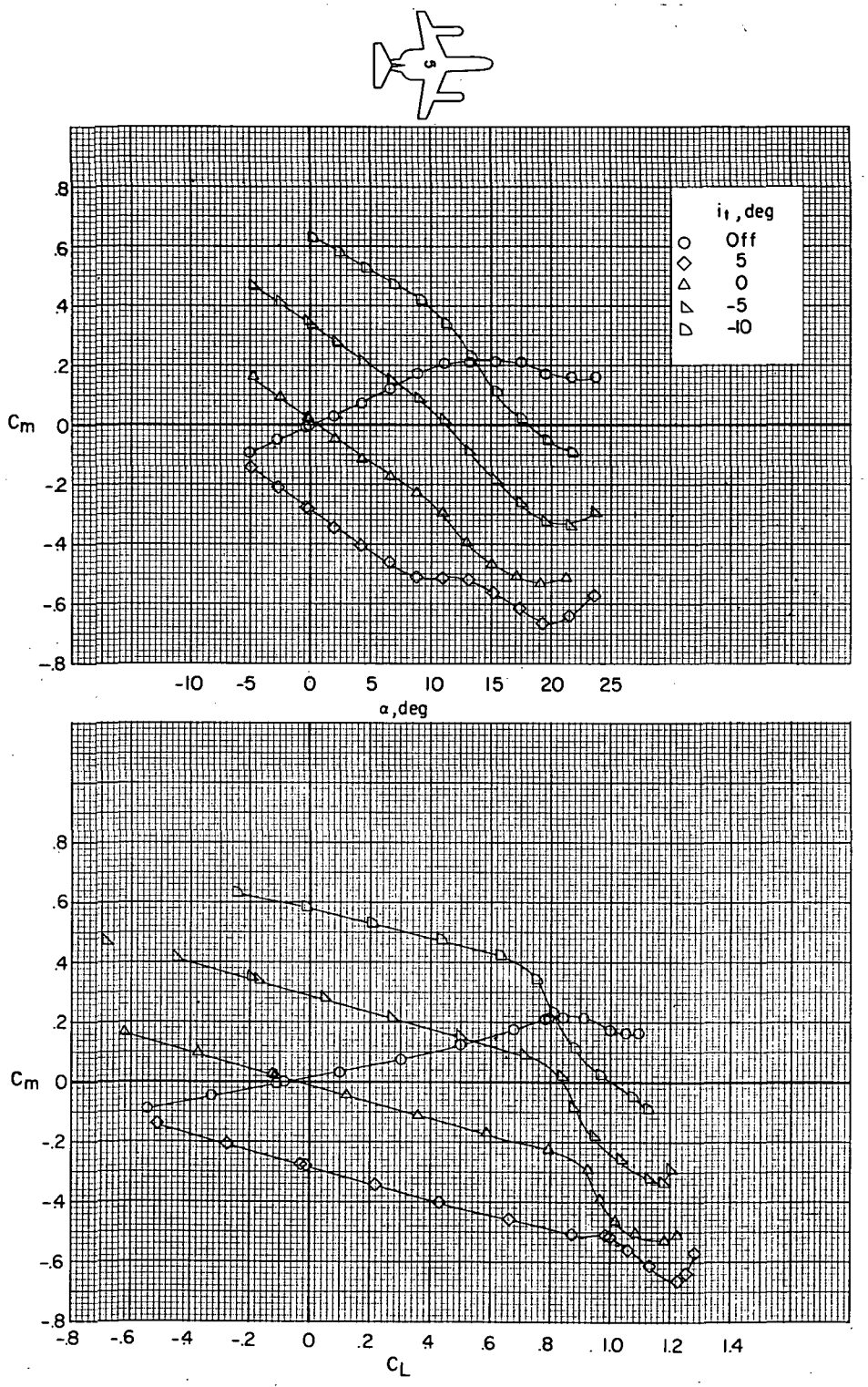

(b) Pitching-moment coefficient.

Figure 10.- Concluded.

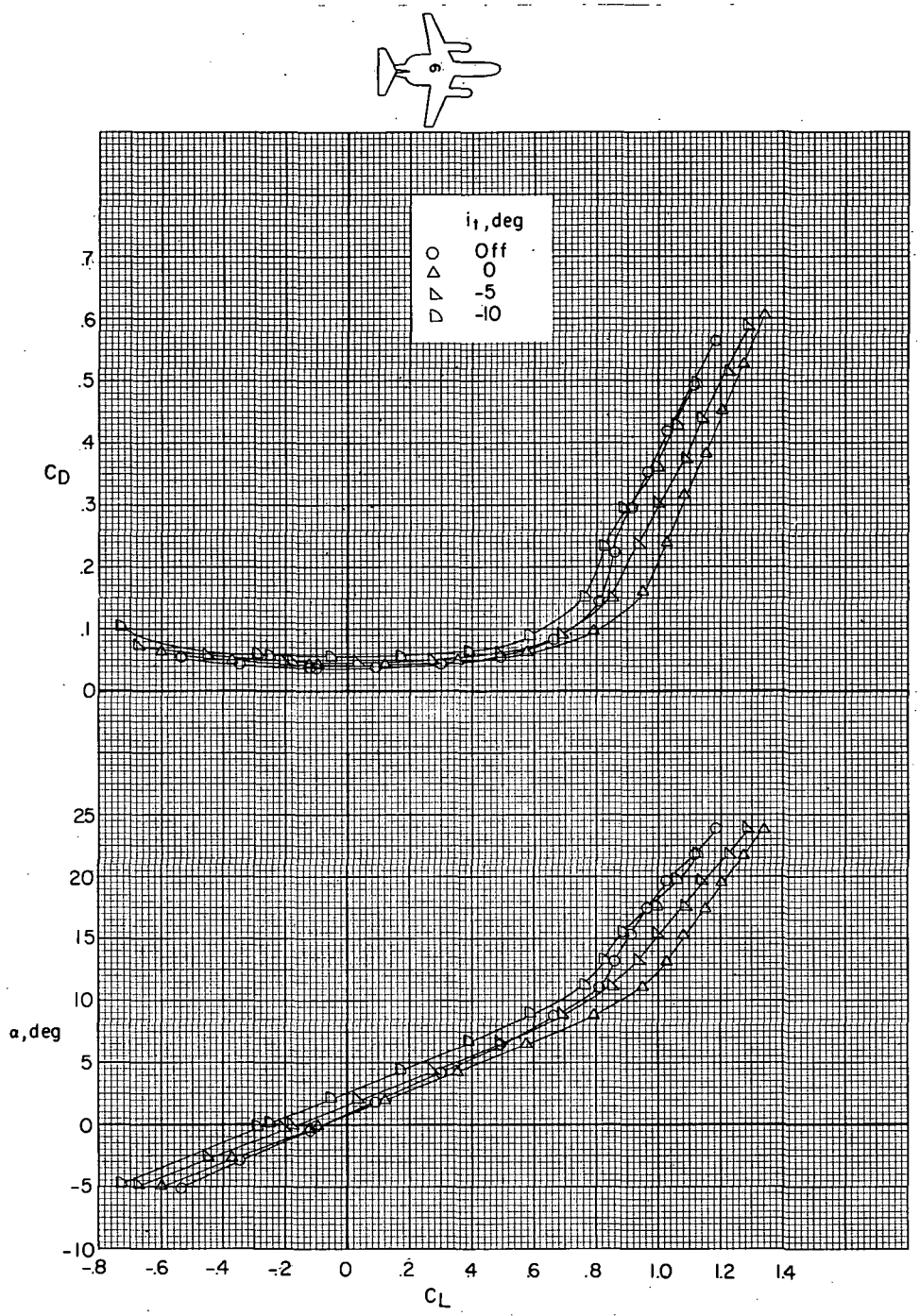

(a) Lift and drag coefficients.

Figure 11.- Effect of horizontal-tail incidence on longitudinal aerodynamic characteristics of configuration 6.

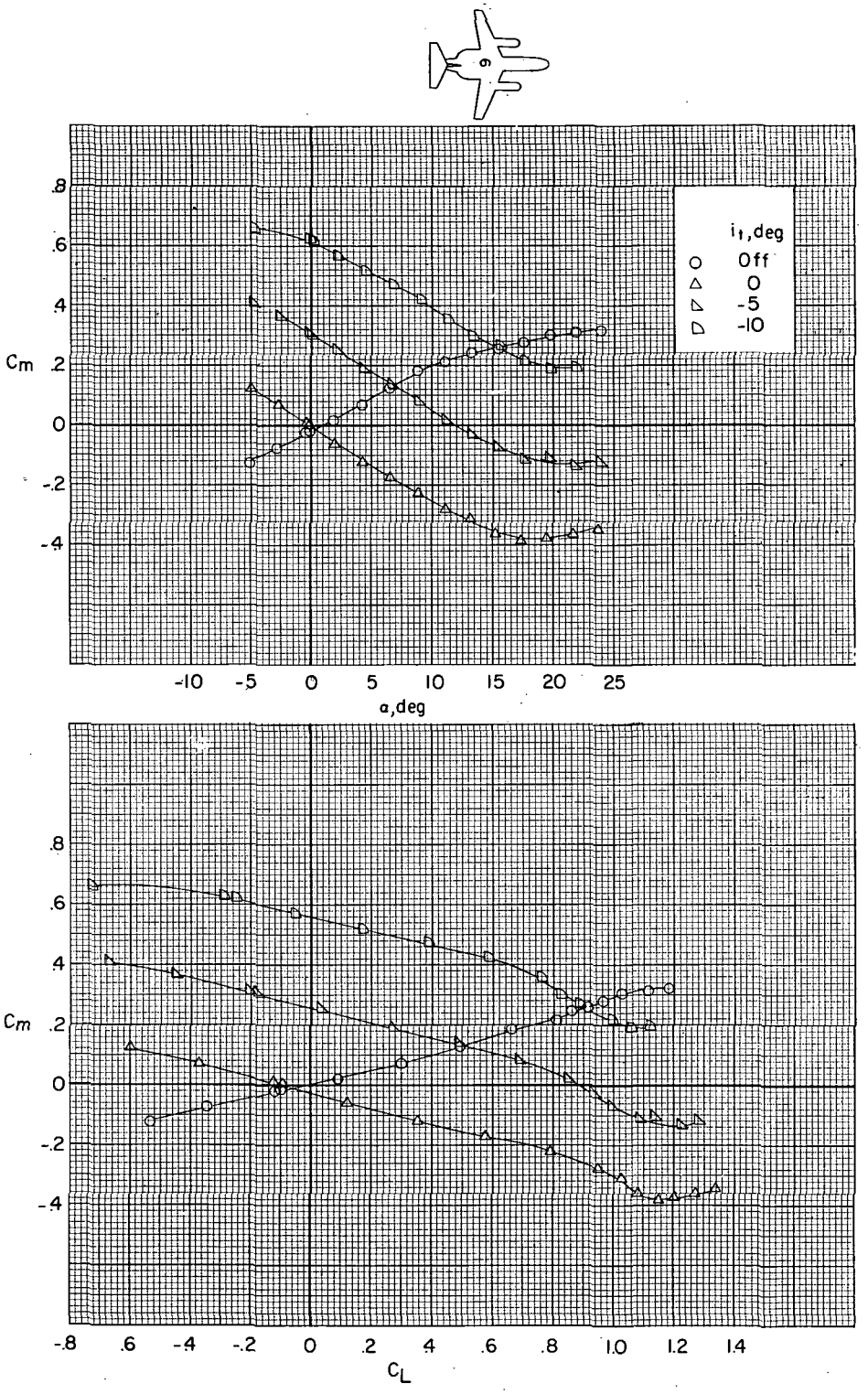

(b) Pitching-moment coefficient.

Figure 11.- Concluded.

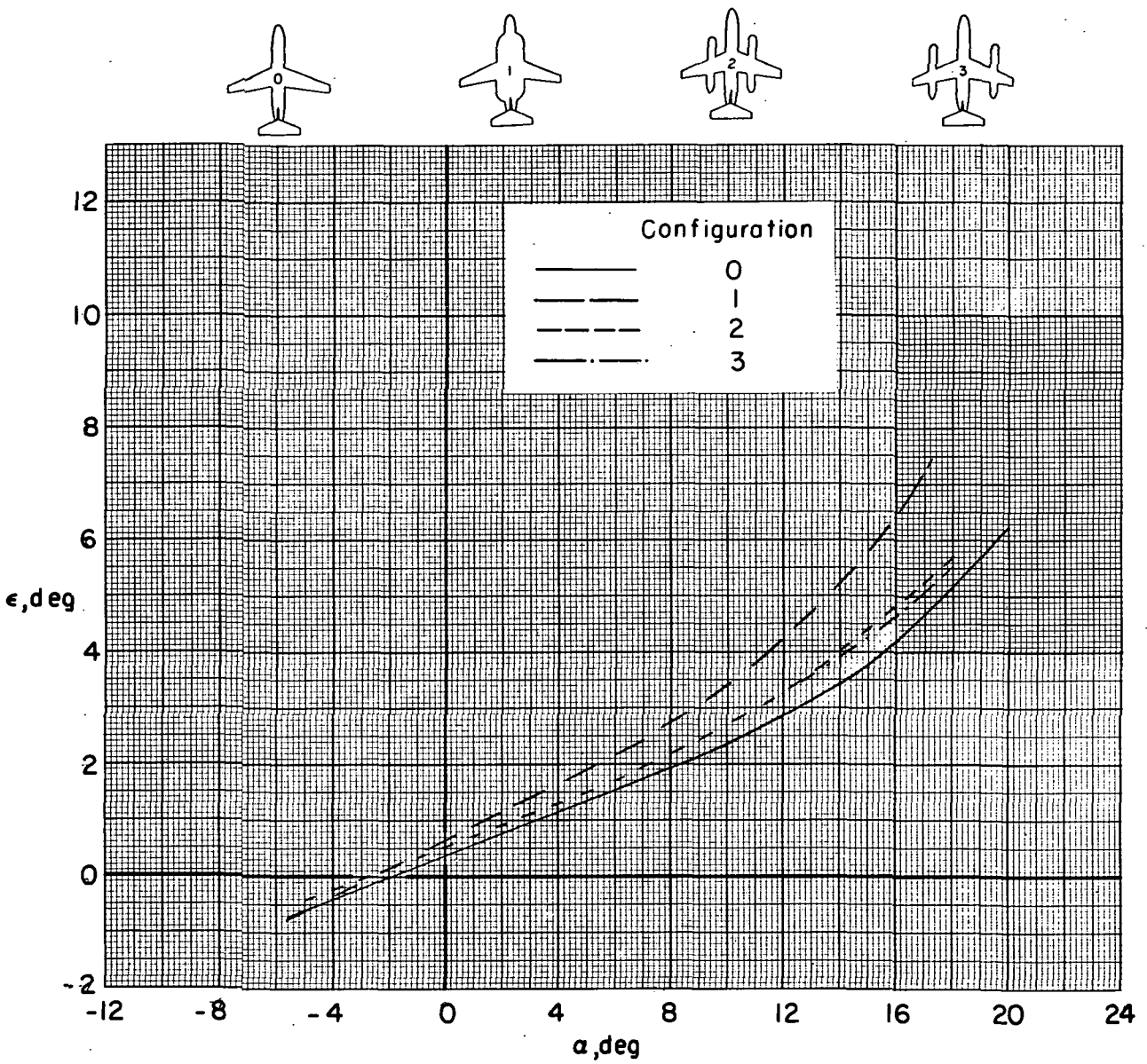

(a) Configurations 0, 1, 2, and 3.

Figure 12.- Comparison of downwash angles at the horizontal tail.

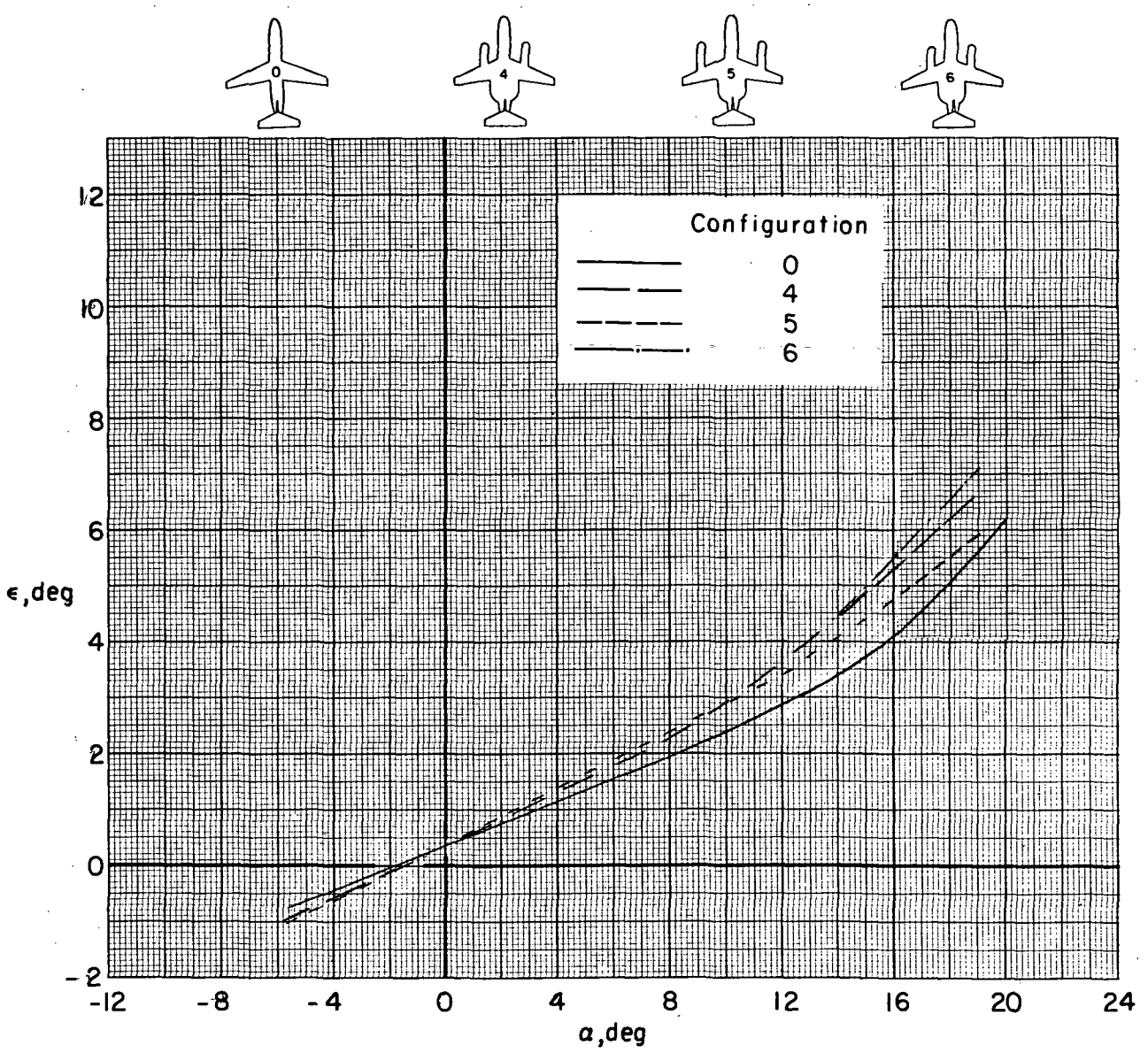

(b) Configurations 0, 4, 5, and 6.

Figure 12.- Concluded.

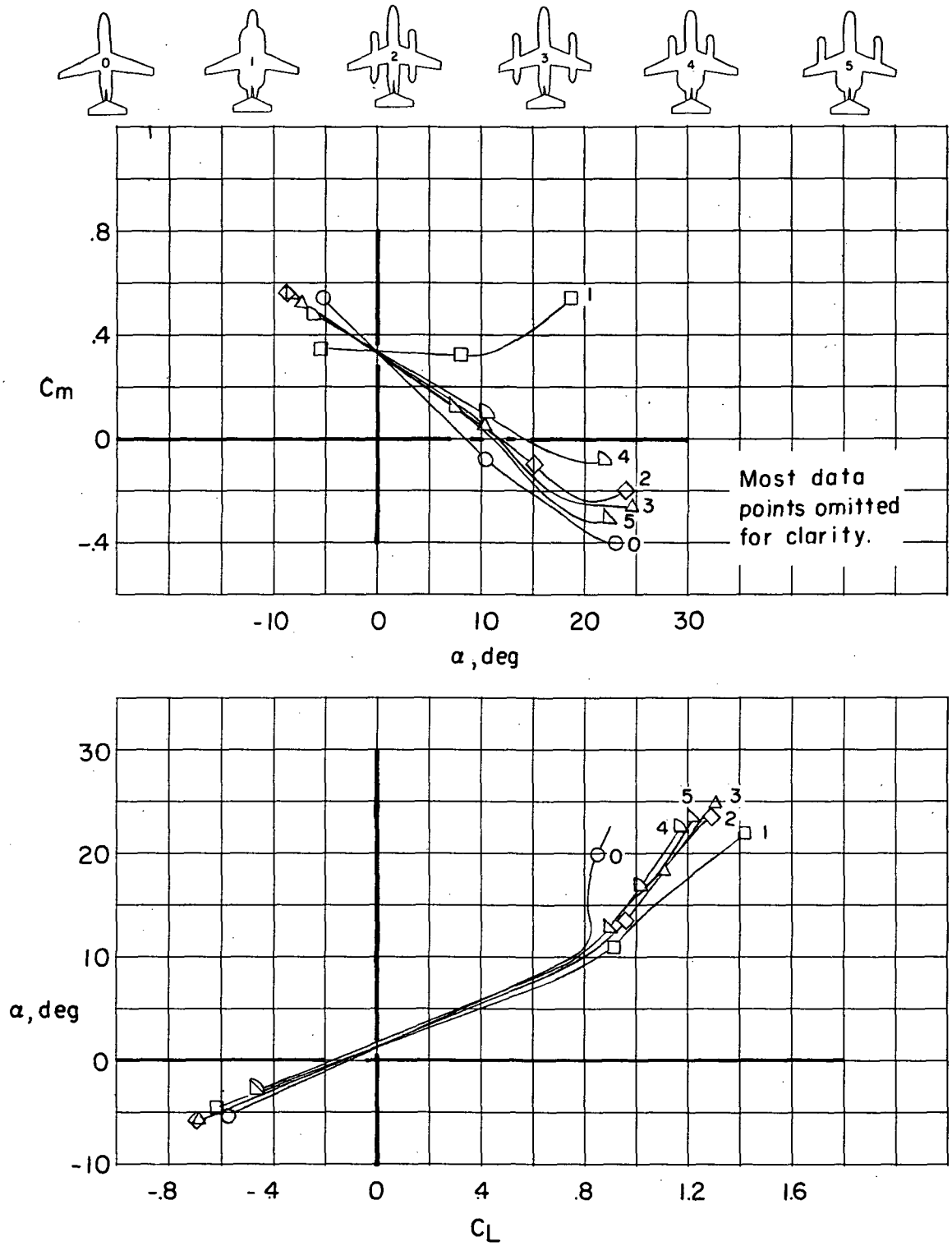

Figure 13.- Comparison of the longitudinal aerodynamic characteristics of configurations 1 to 5. $i_t = -5^o$; $\bar{x} = 0.25\bar{c}$.

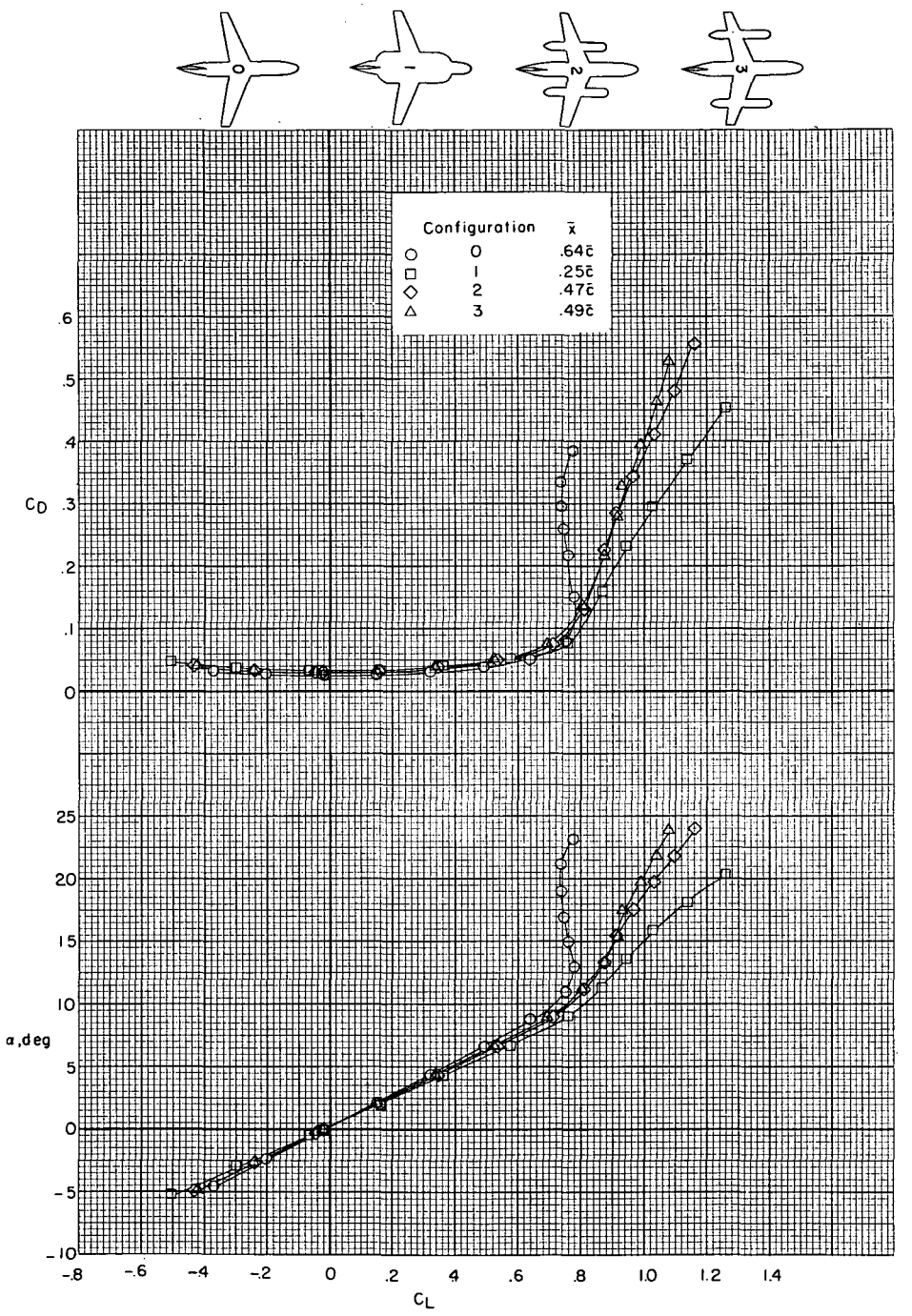

(a) Lift and drag coefficients with horizontal tail off.

Figure 14.- Comparison of longitudinal aerodynamic characteristics of configurations 0, 1, 2, and 3 at $\partial C_m/\partial C_L = -0.05$.

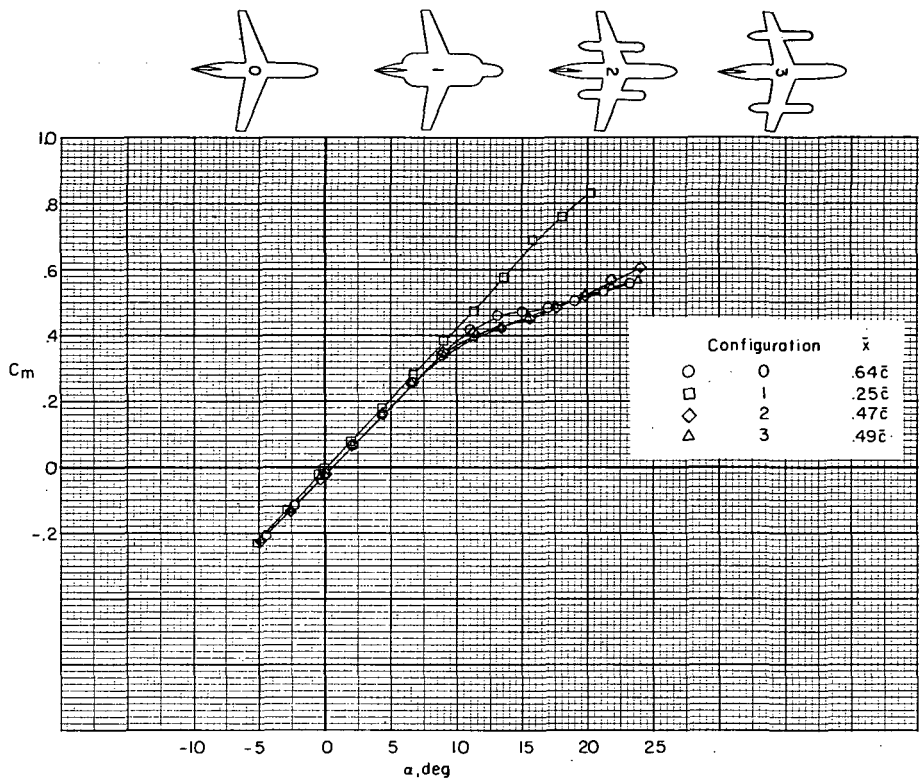

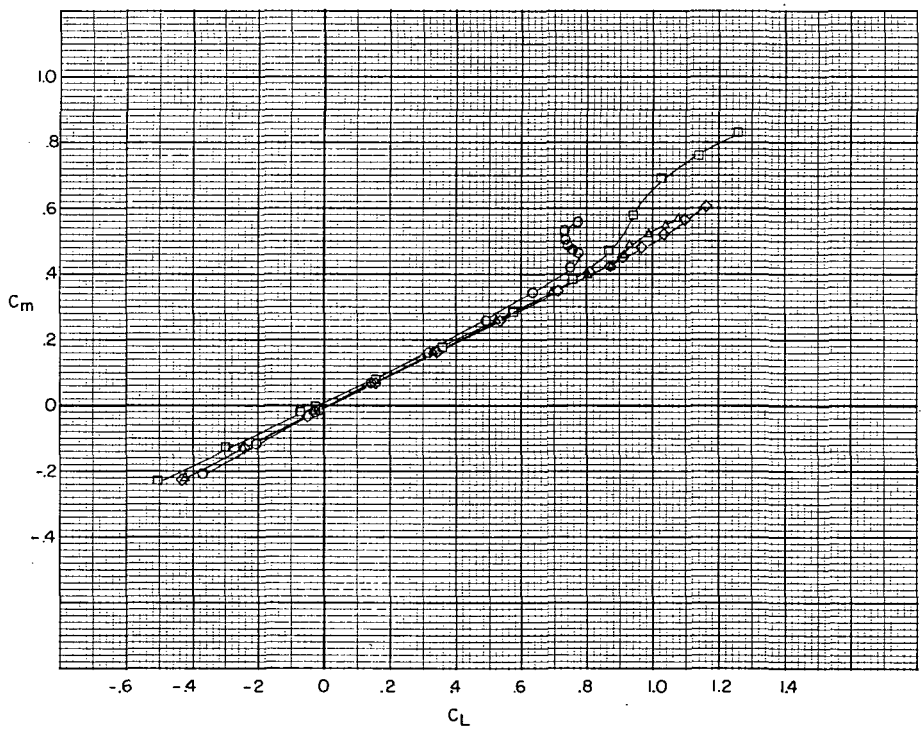

(b) Pitching-moment coefficients with horizontal tail off.

Figure 14.- Continued.

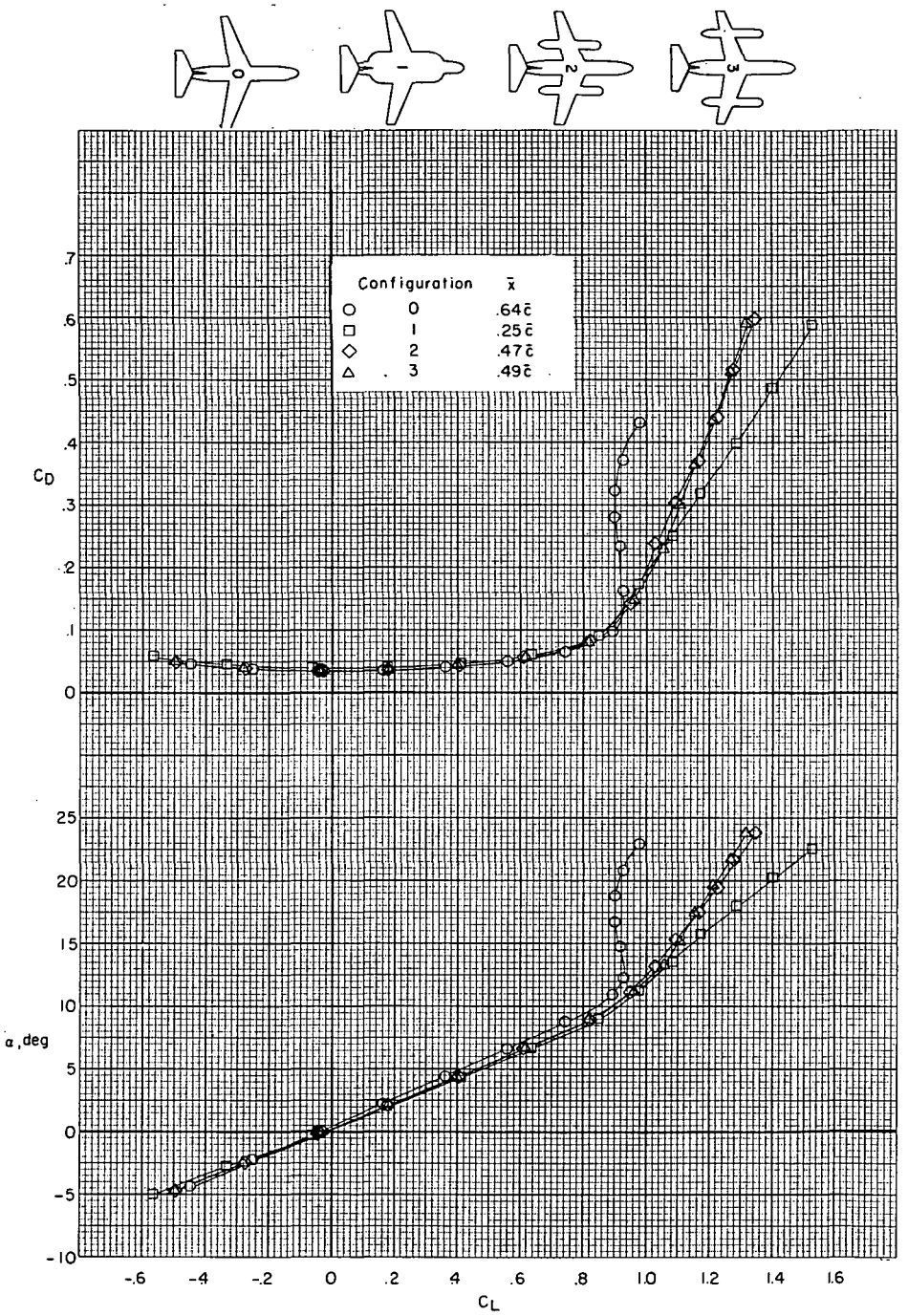

(c) Lift and drag coefficients with $i_t = 0^o$.

Figure 14.- Continued.

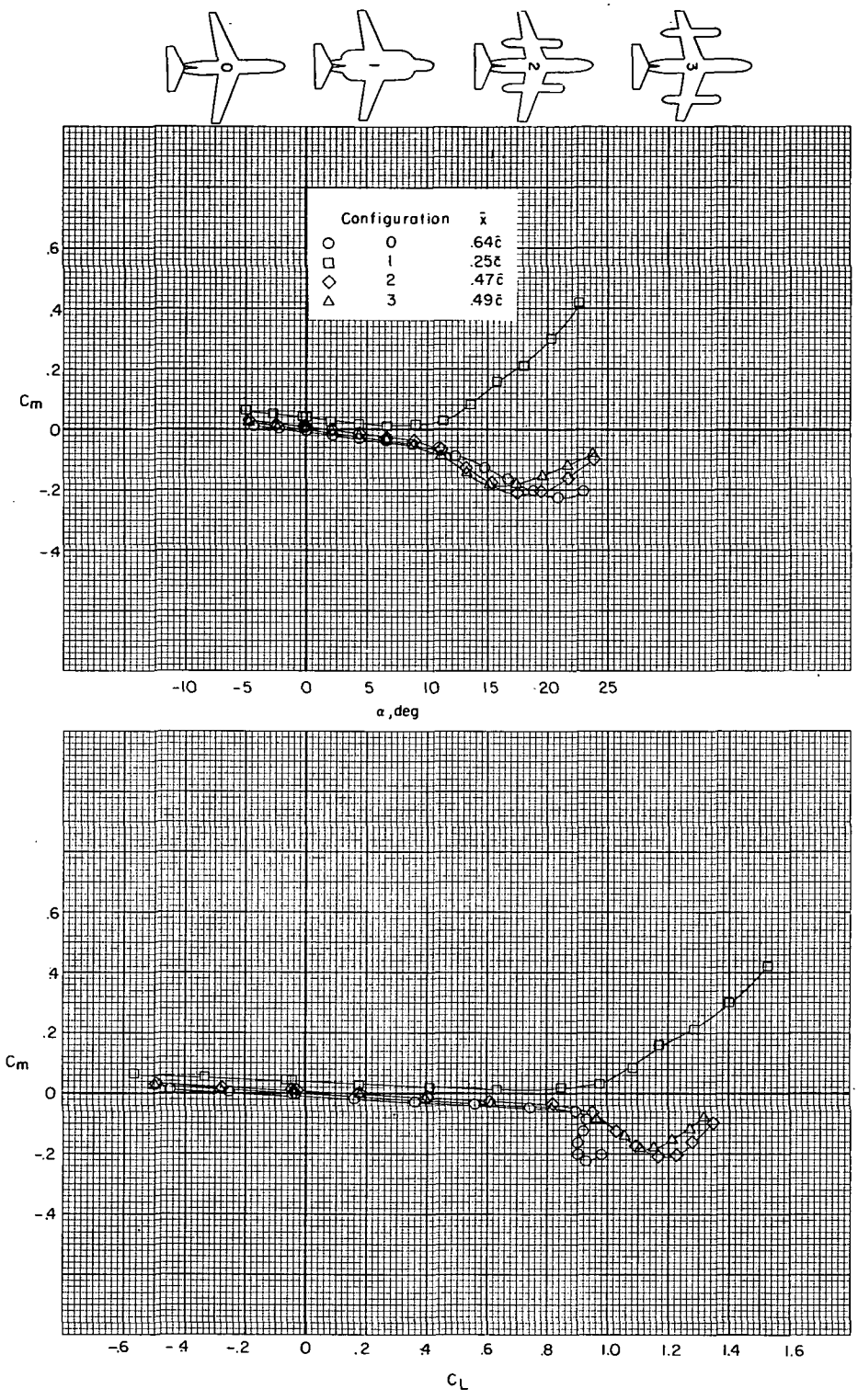

(d) Pitching-moment coefficients with $i_t = 0^o$.

Figure 14.- Concluded.

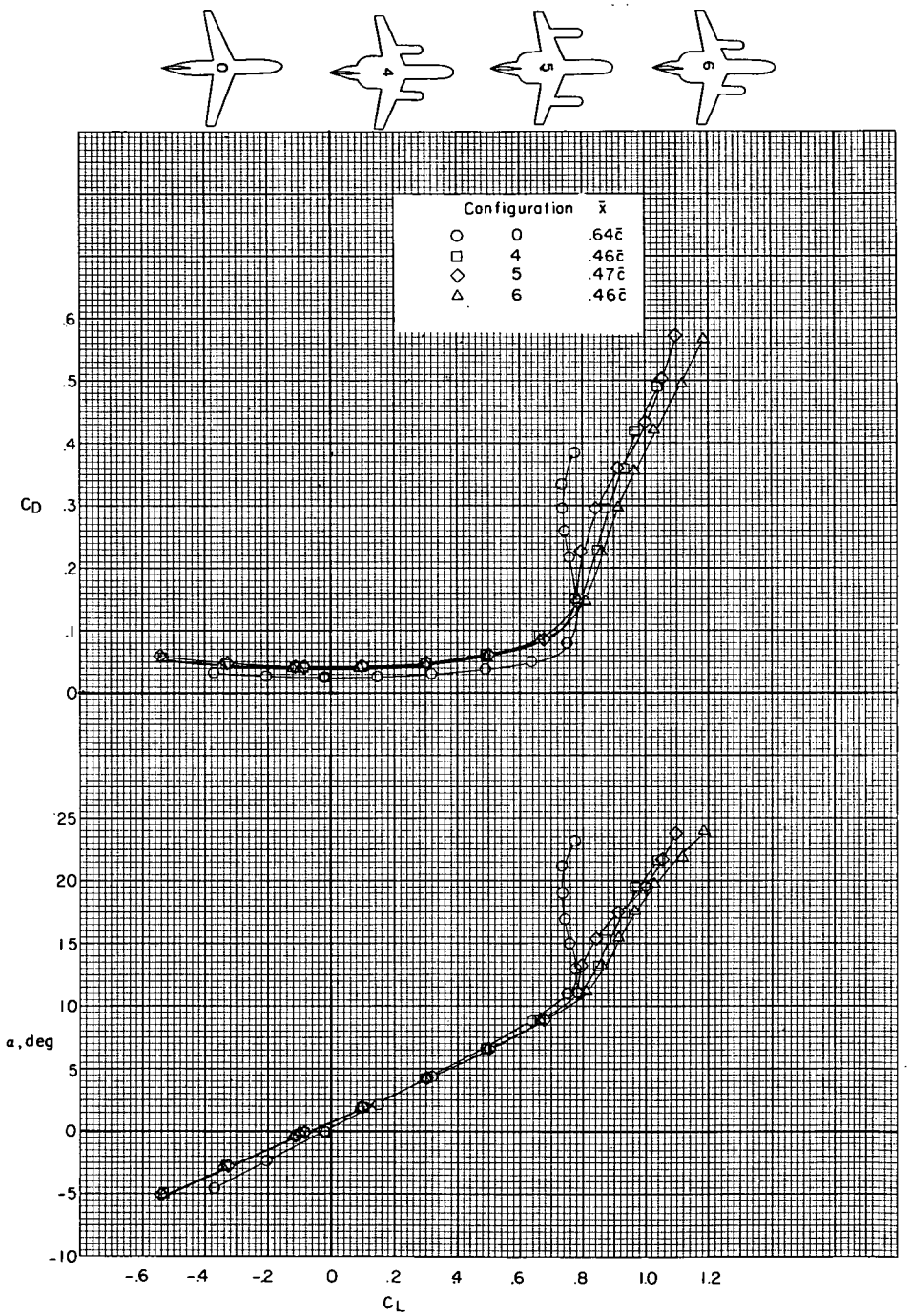

(a) Lift and drag coefficients with horizontal tail off.

Figure 15.- Comparison of longitudinal aerodynamic characteristics of configurations 0, 4, 5, and 6 at $\partial C_m/\partial C_L = -0.05$.

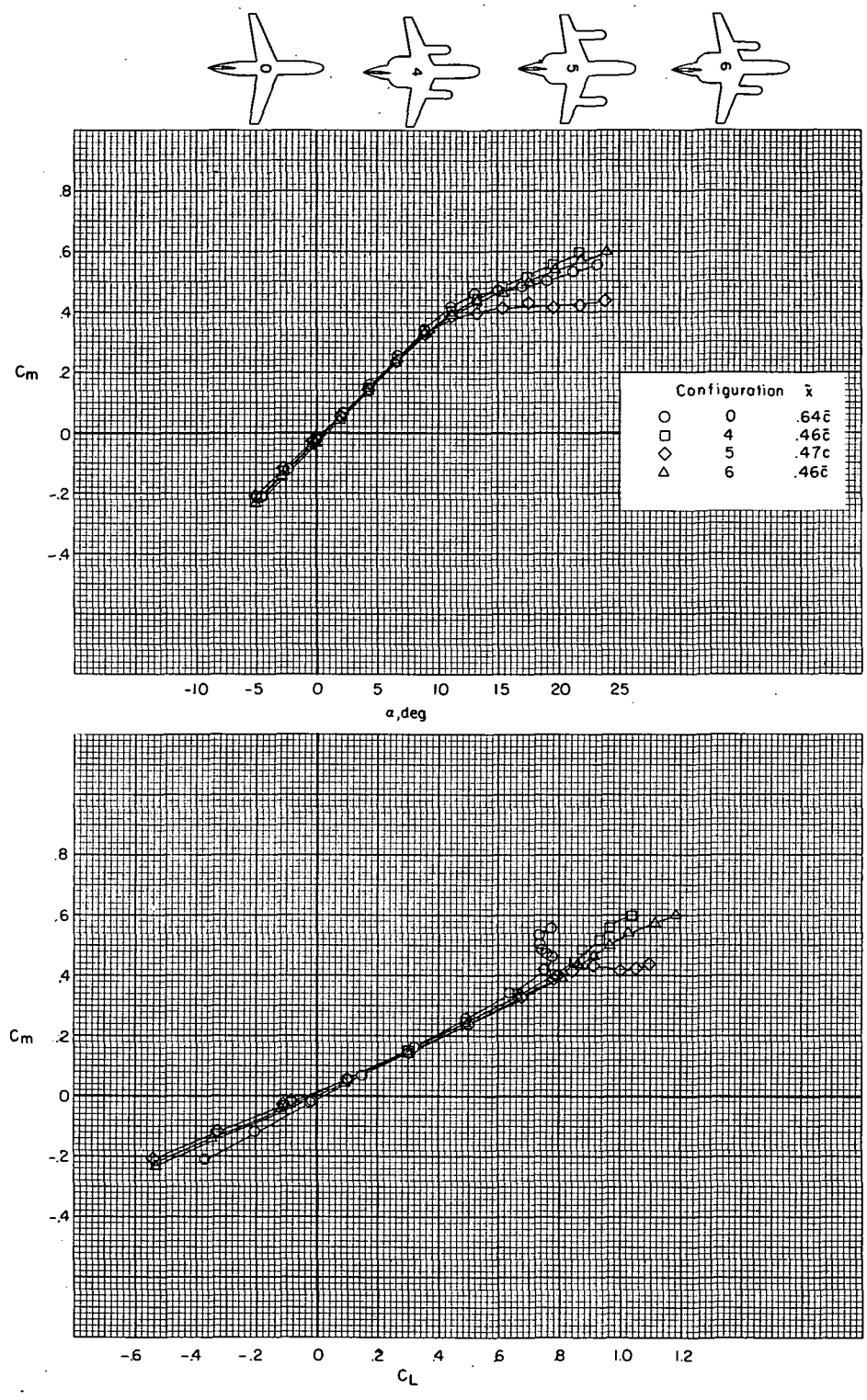

(b) Pitching-moment coefficients with horizontal tail off.

Figure 15.- Continued.

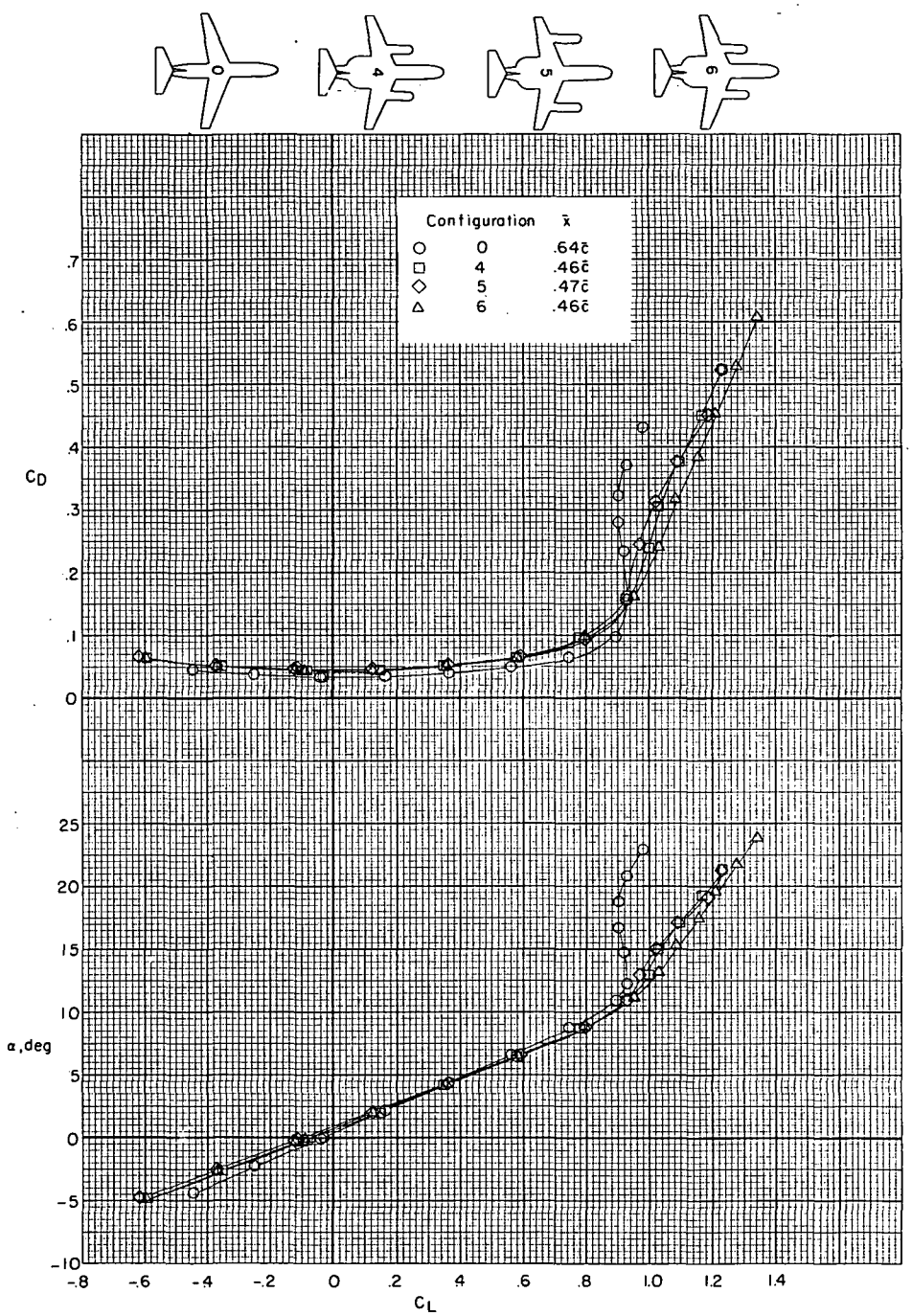

(c) Lift and drag coefficients with $i_t = 0^o$.

Figure 15.- Continued.

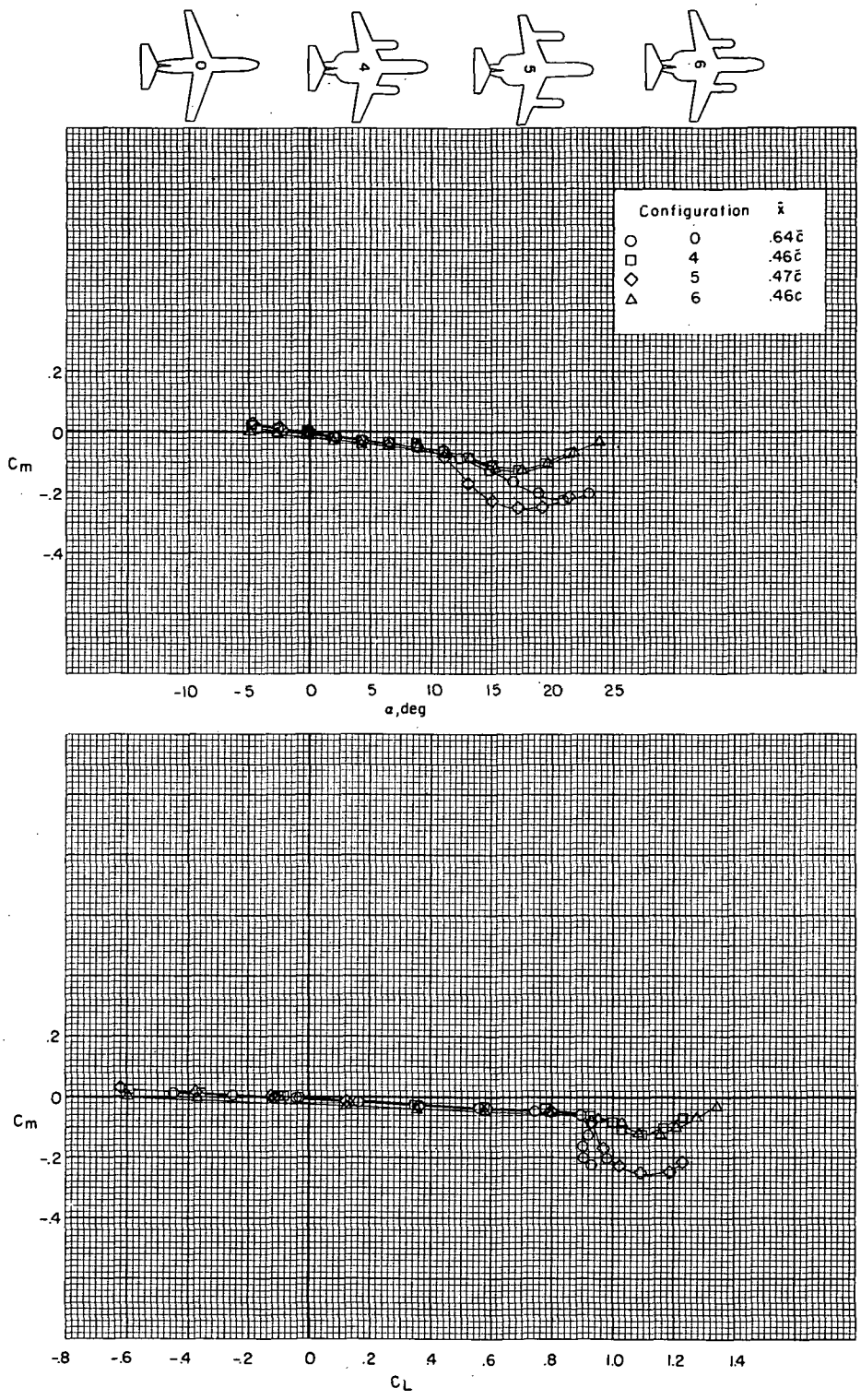

(d) Pitching-moment coefficients with $i_t = 0^o$.

Figure 15.- Concluded.

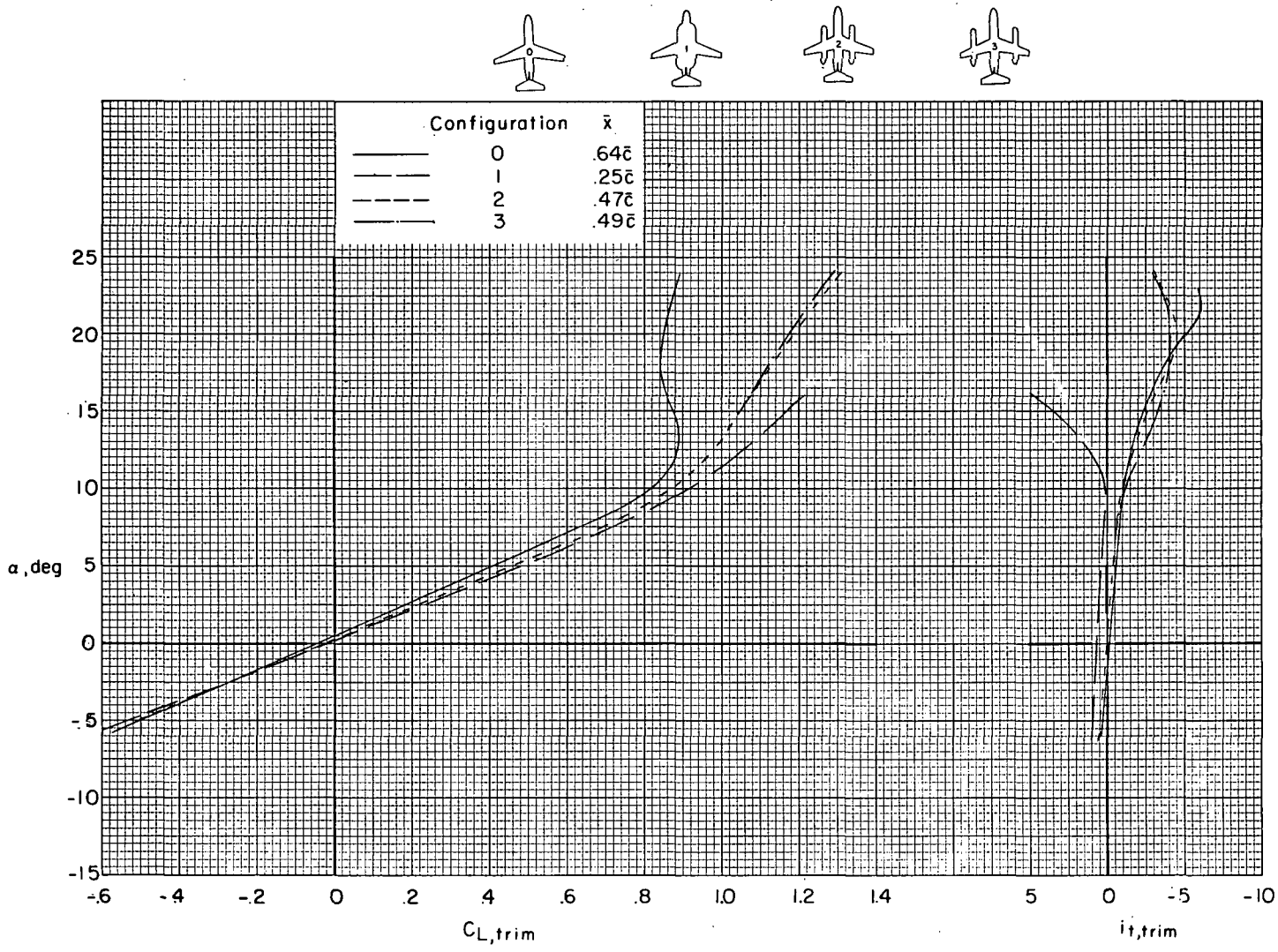

(a) Lift coefficients.

Figure 16.- Comparison of trimmed lift and drag coefficients of configurations 0, 1, 2, and 3.

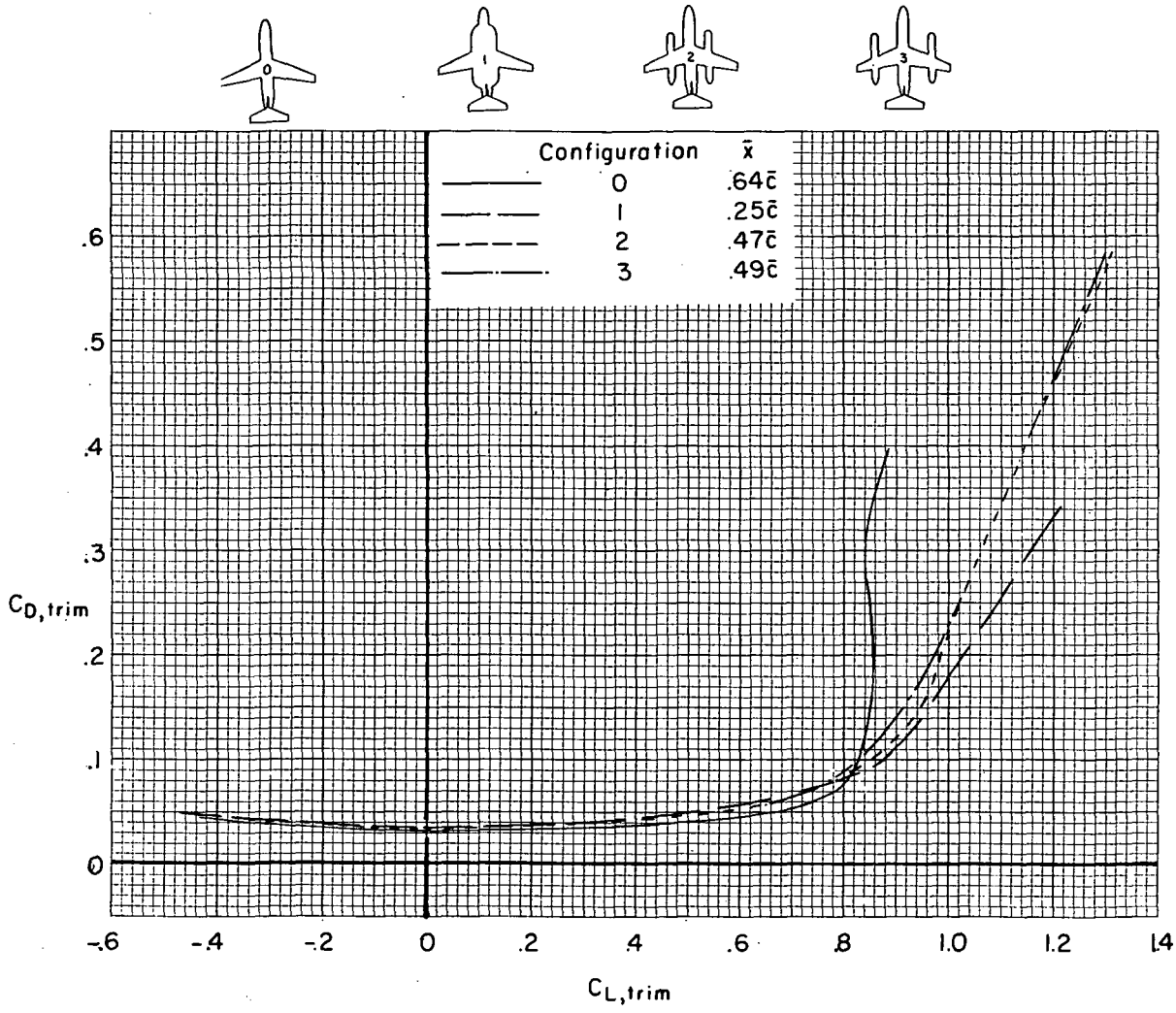

(b) Drag coefficients.

Figure 16.- Concluded.

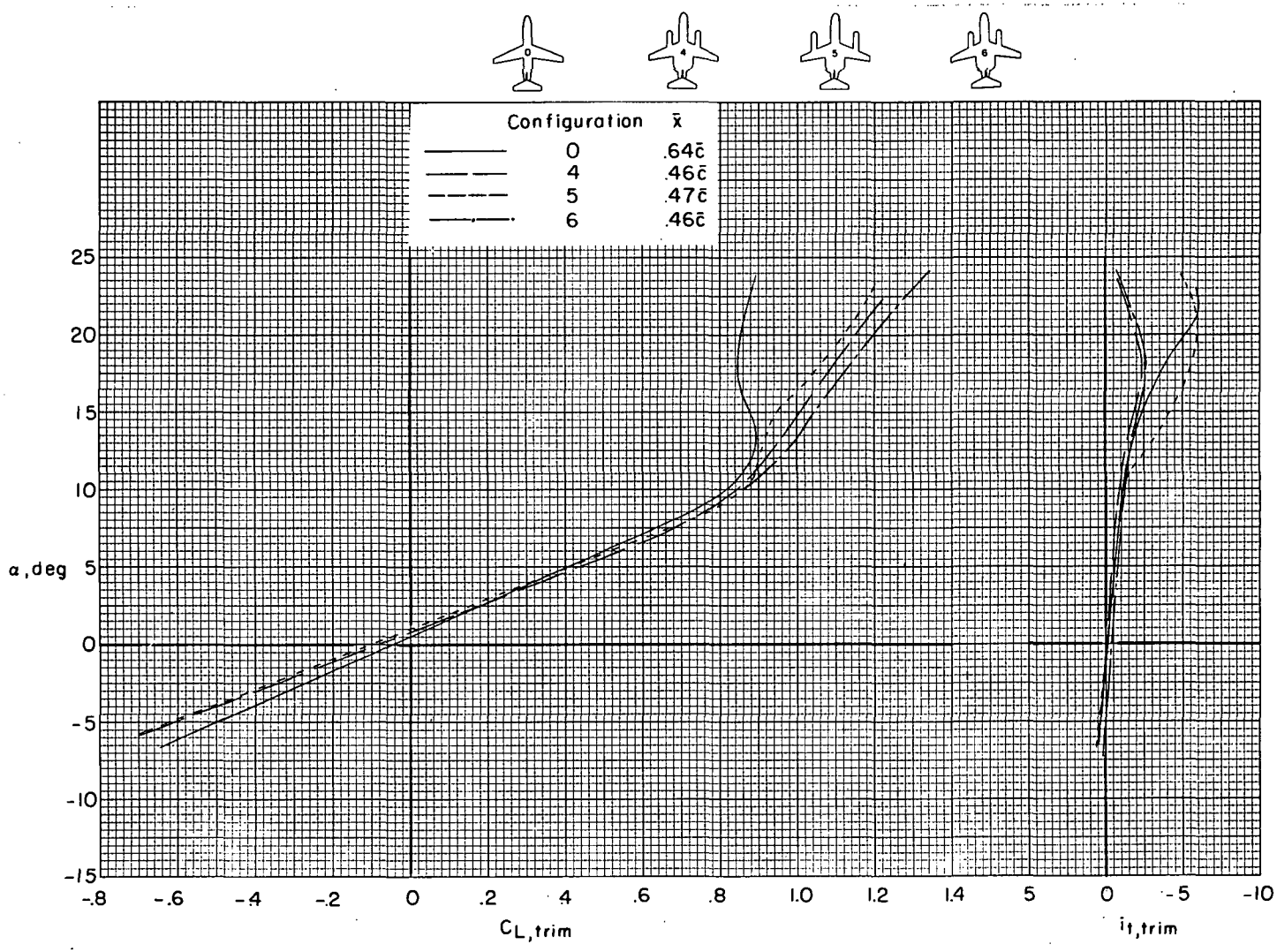

(a) Lift coefficients.

Figure 17.- Comparison of trimmed lift and drag coefficients of configurations 0, 4, 5, and 6.

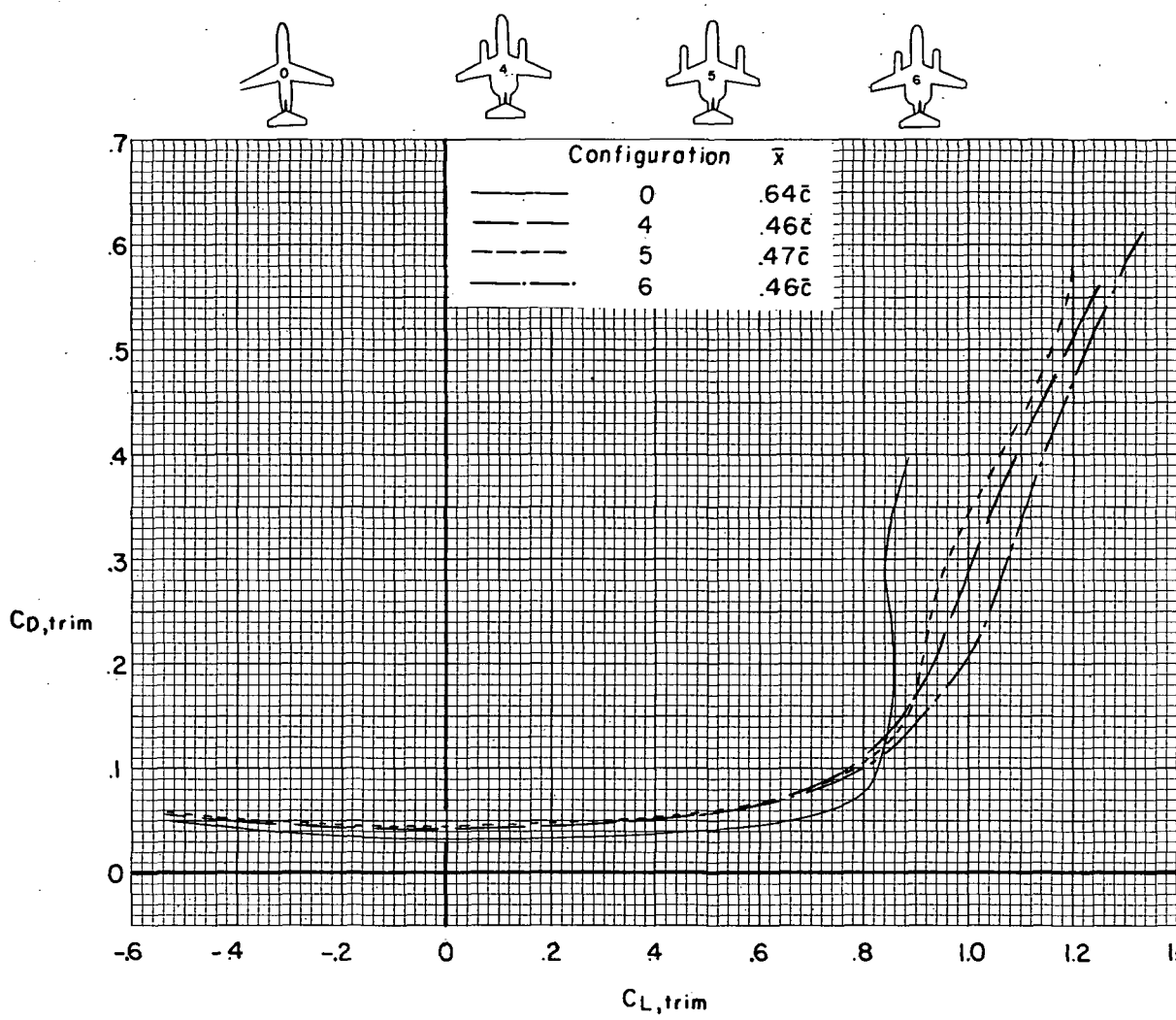

(b) Drag coefficients.

Figure 17.- Concluded.

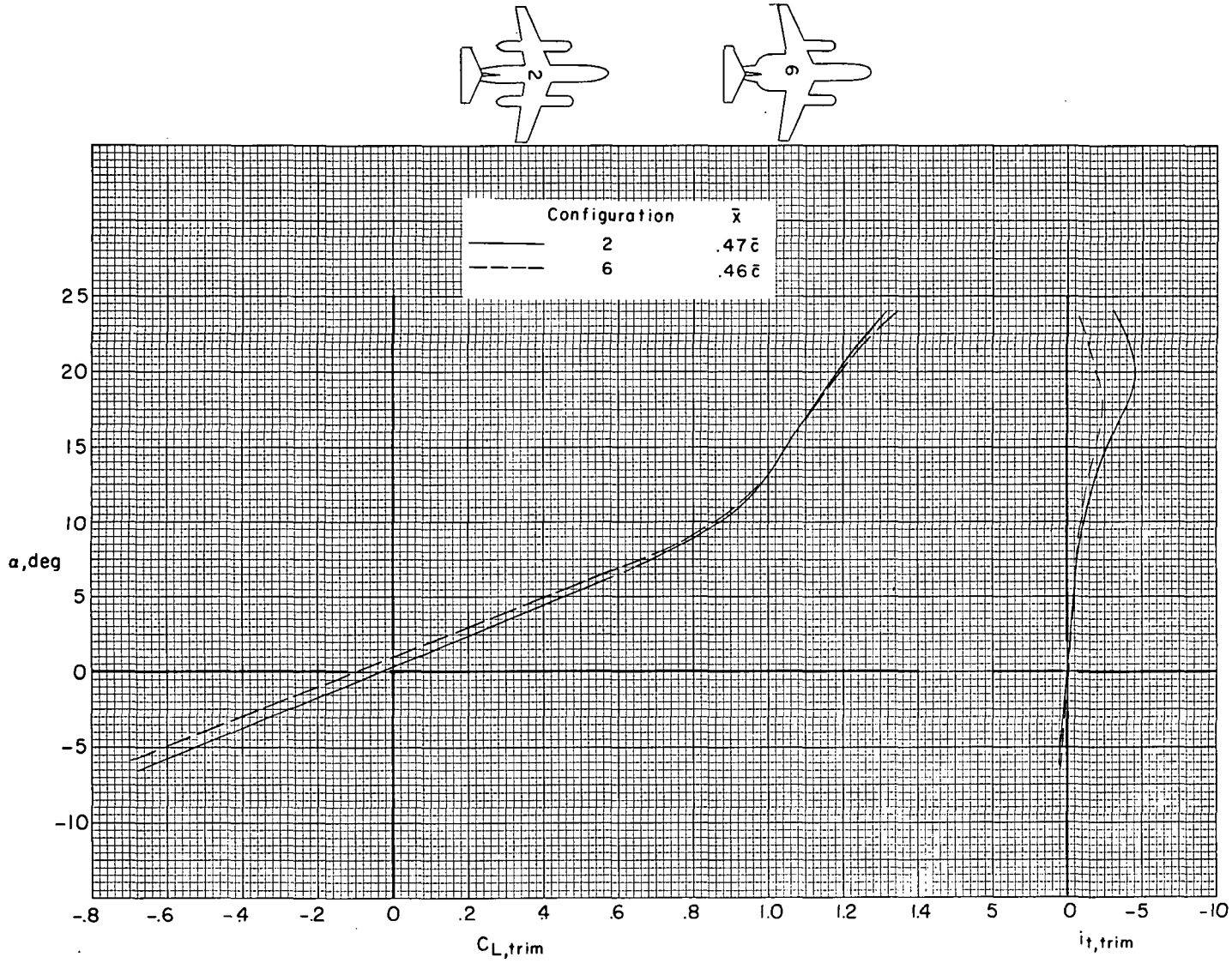

(a) Lift coefficients.

Figure 18.- Comparison of trimmed lift and drag coefficients of the best in-line pod and the best split pod configuration.

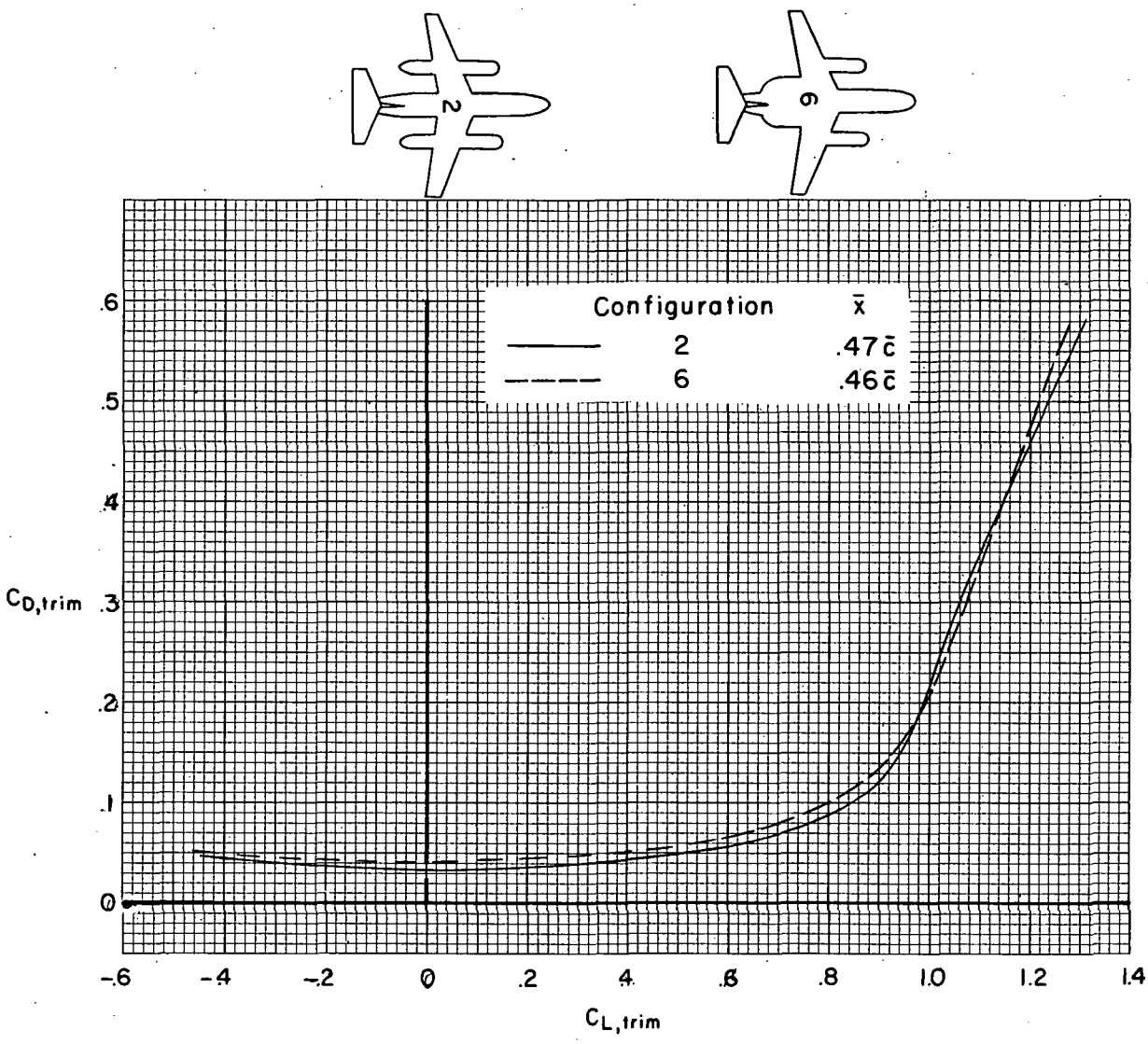

(b) Drag coefficients.

Figure 18.- Concluded.

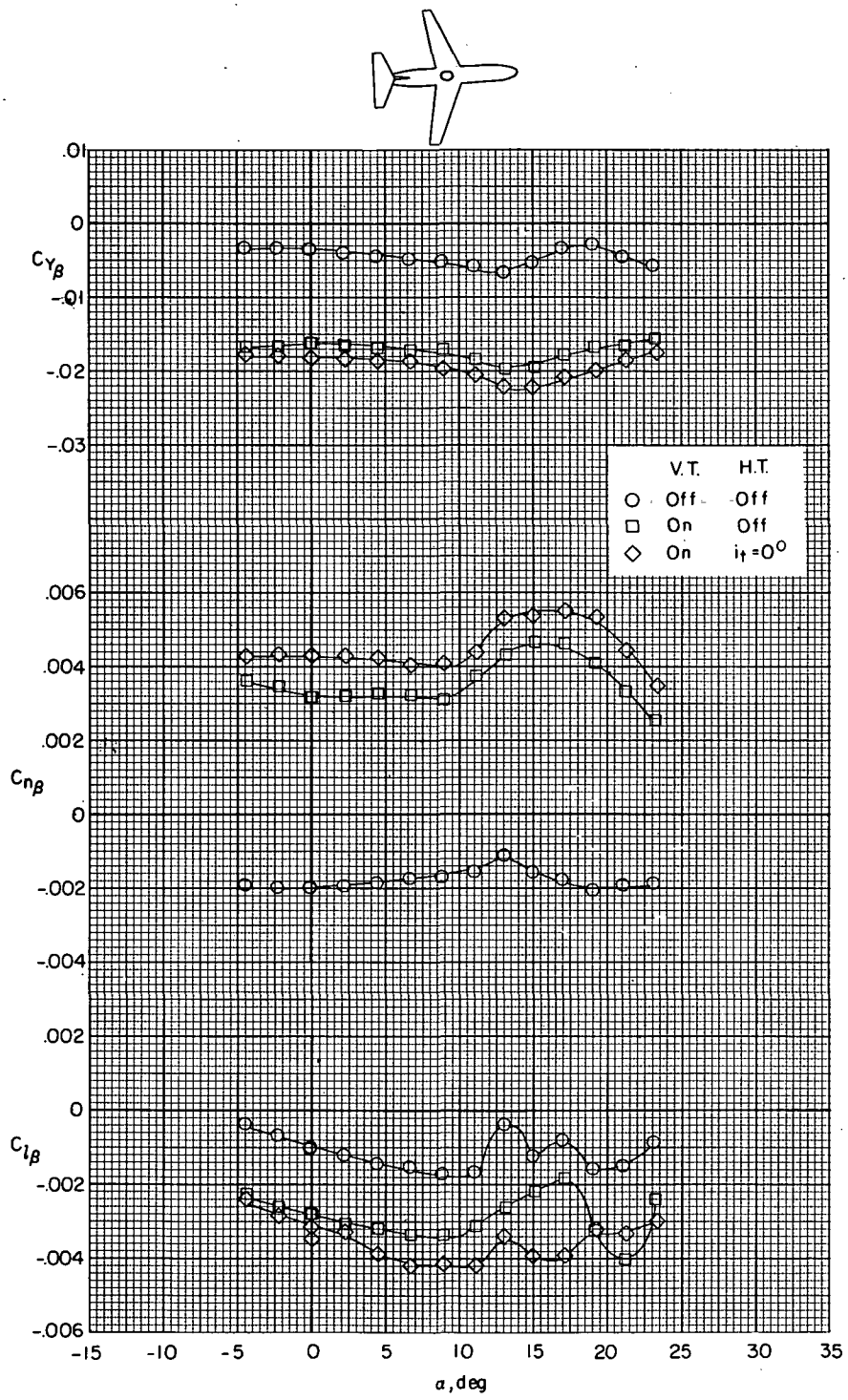

(a) Configuration 0.

Figure 19.- Effect of empennage on lateral-stability derivatives with $\bar{x} = 0.25\bar{c}$.

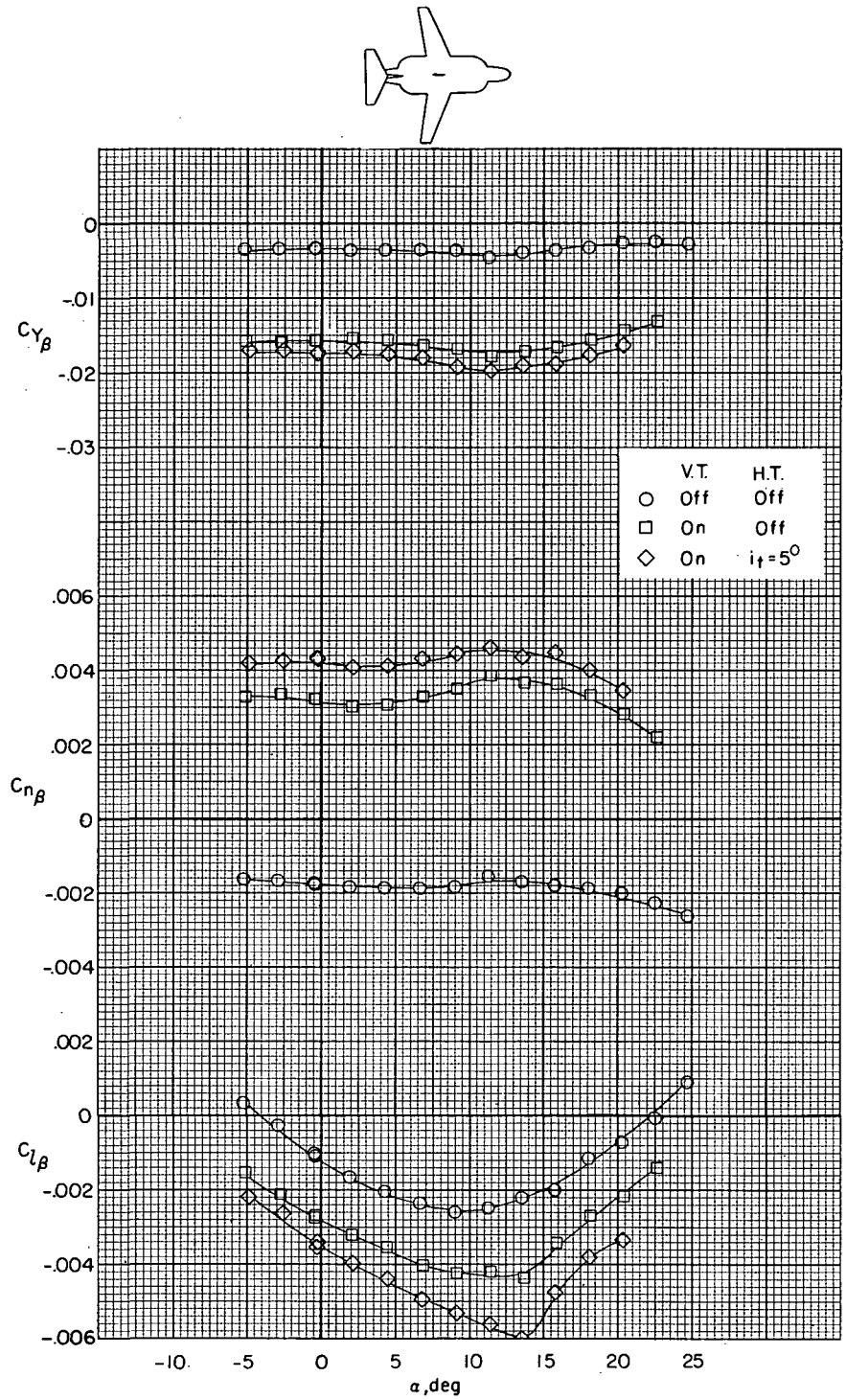

(b) Configuration 1.

Figure 19.- Continued.

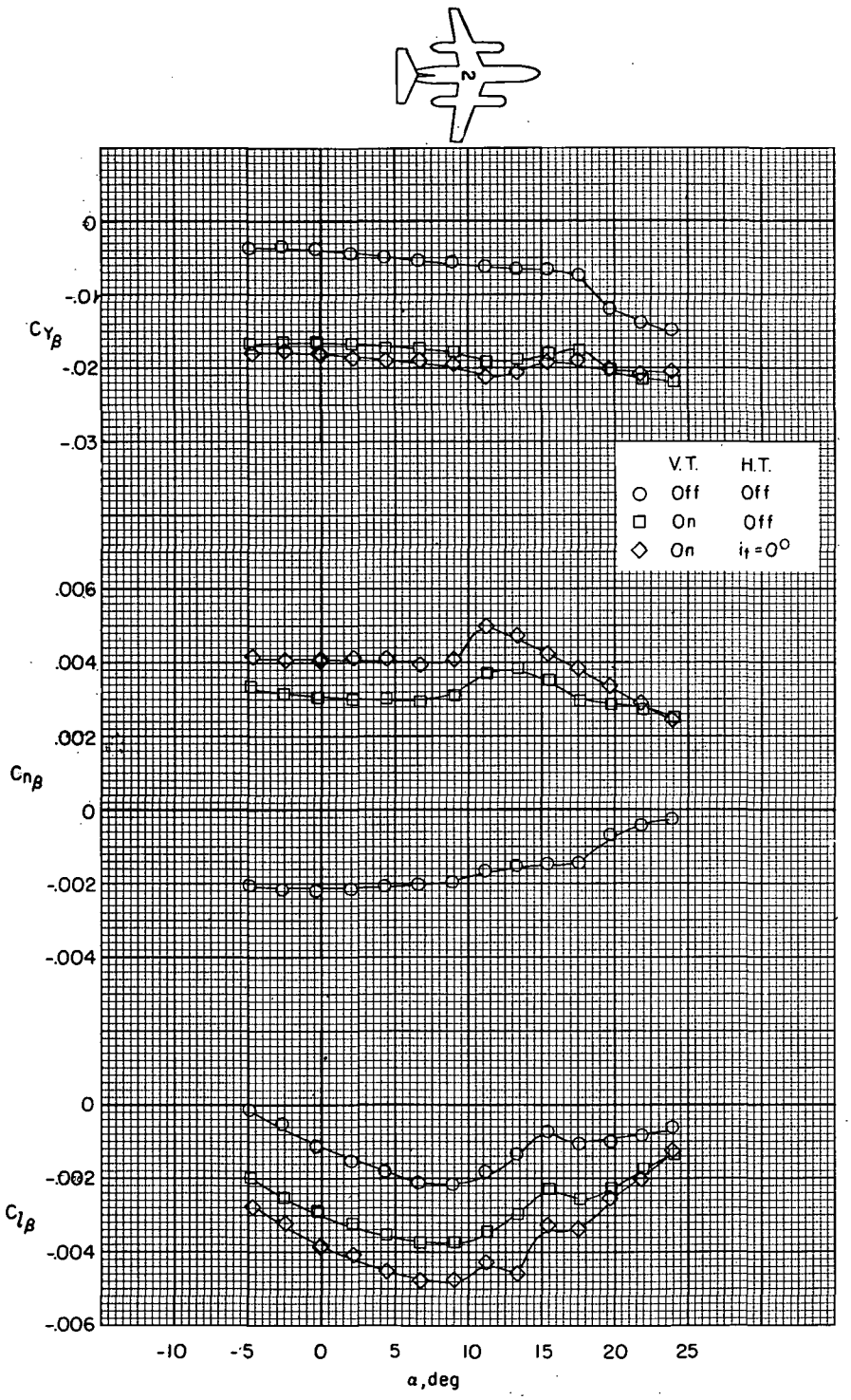

(c) Configuration 2.

Figure 19.- Continued.

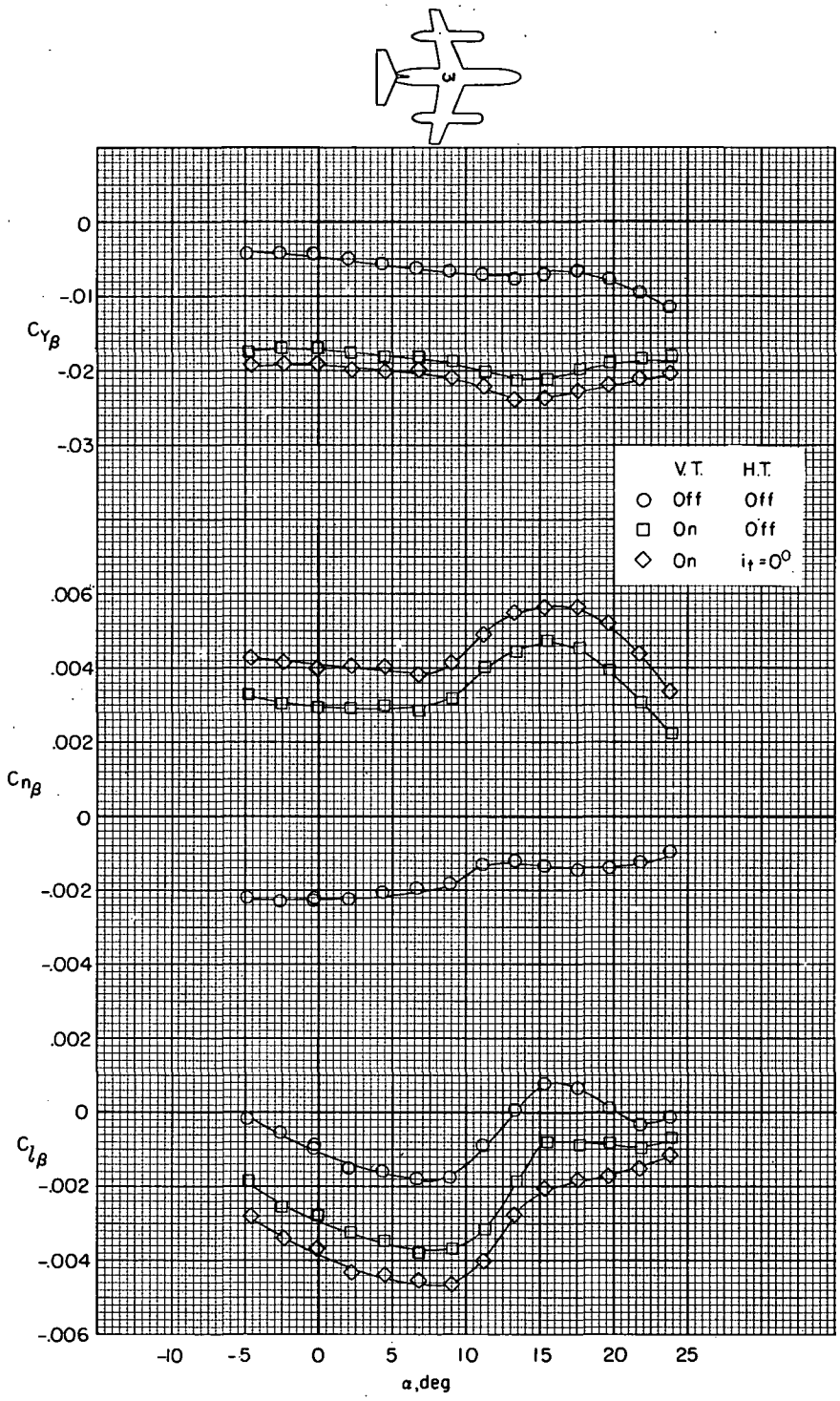

(d) Configuration 3.

Figure 19.- Continued.

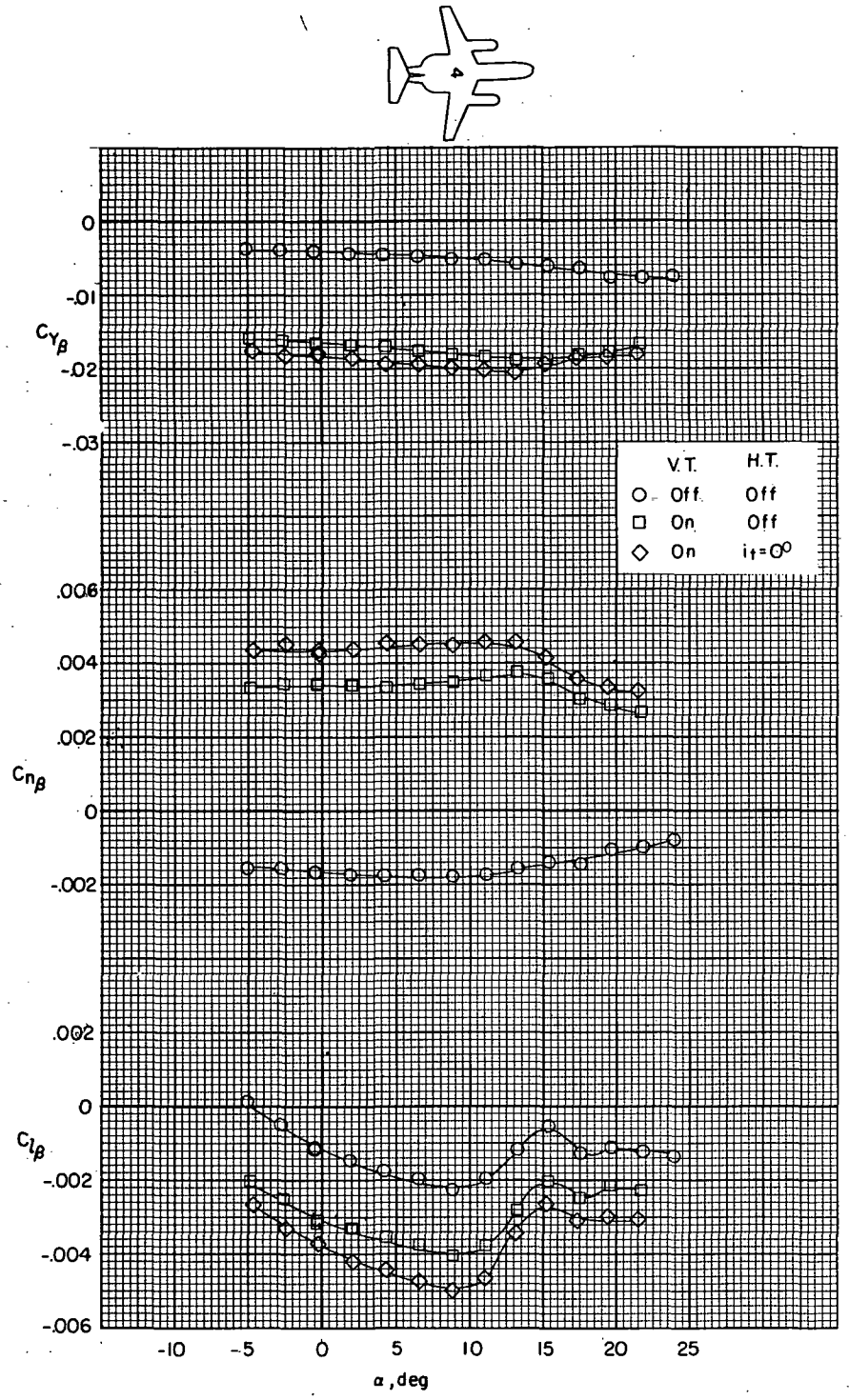

(e) Configuration 4.

Figure 19.- Continued.

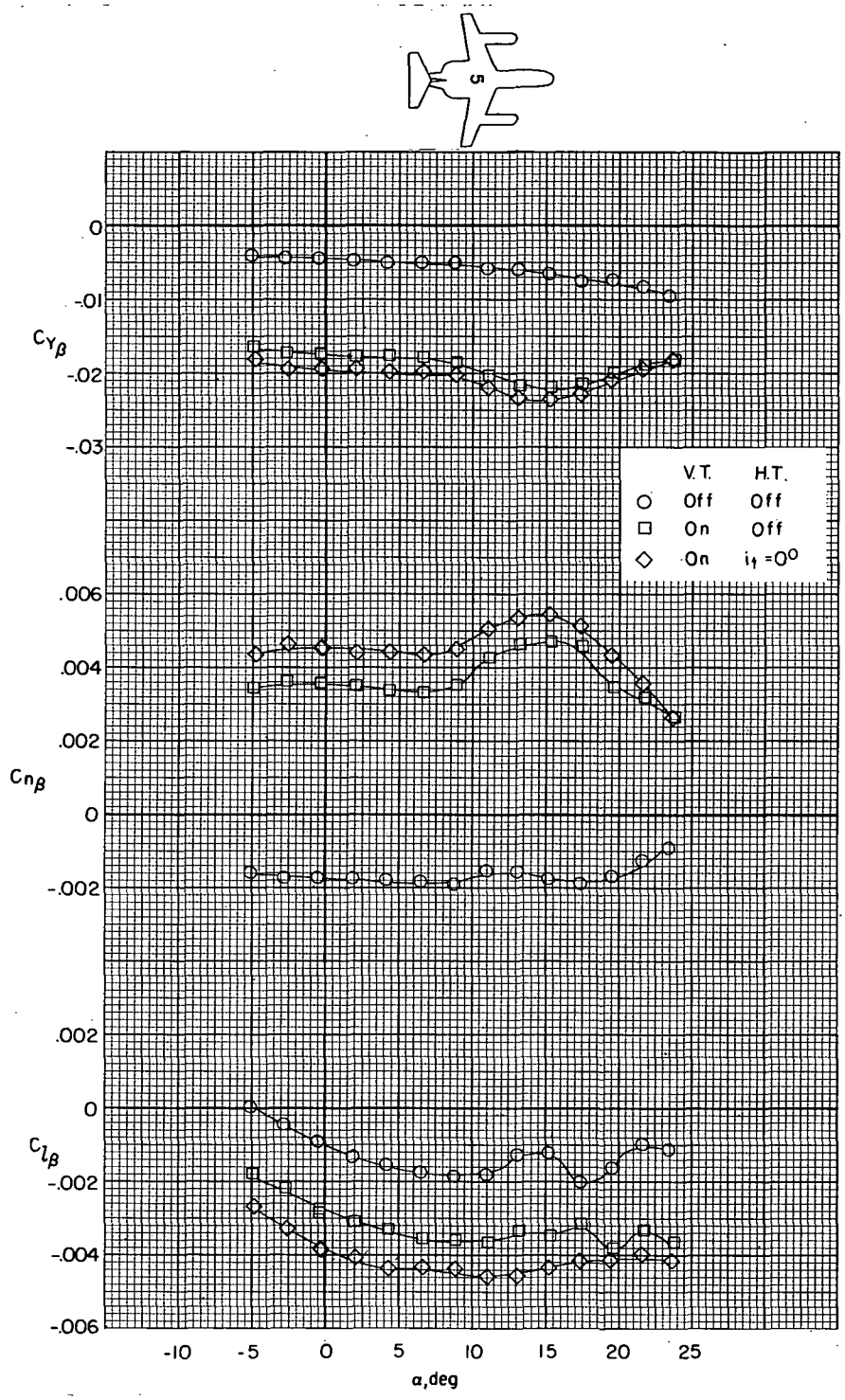

(f) Configuration 5.

Figure 19.- Concluded.

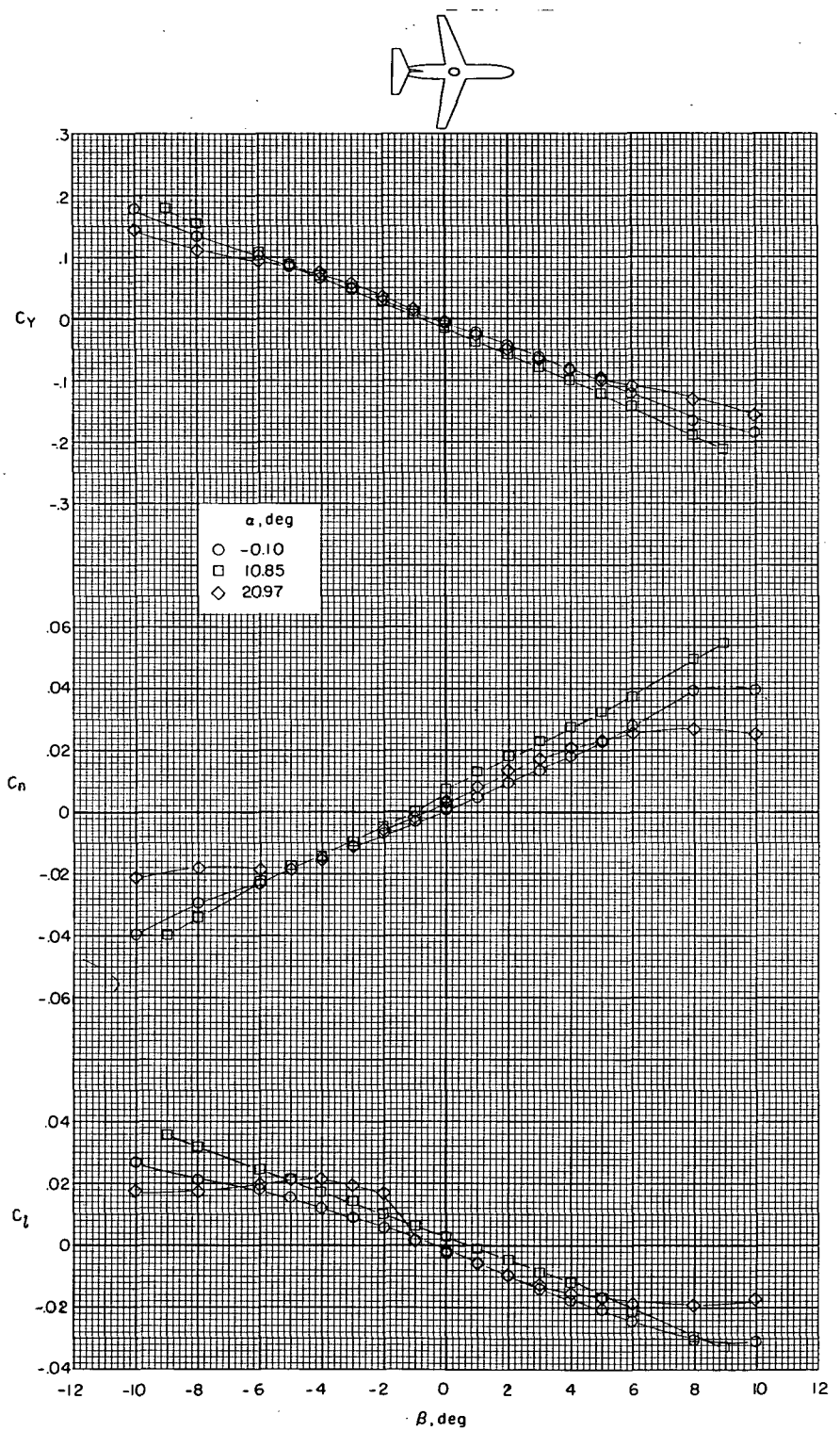

(a) Configuration 0, $i_t = 5^o$.

Figure 20.- Variation of lateral-directional characteristics with angle of sideslip for $\alpha \approx 0^o$, 10^o, and 20^o.

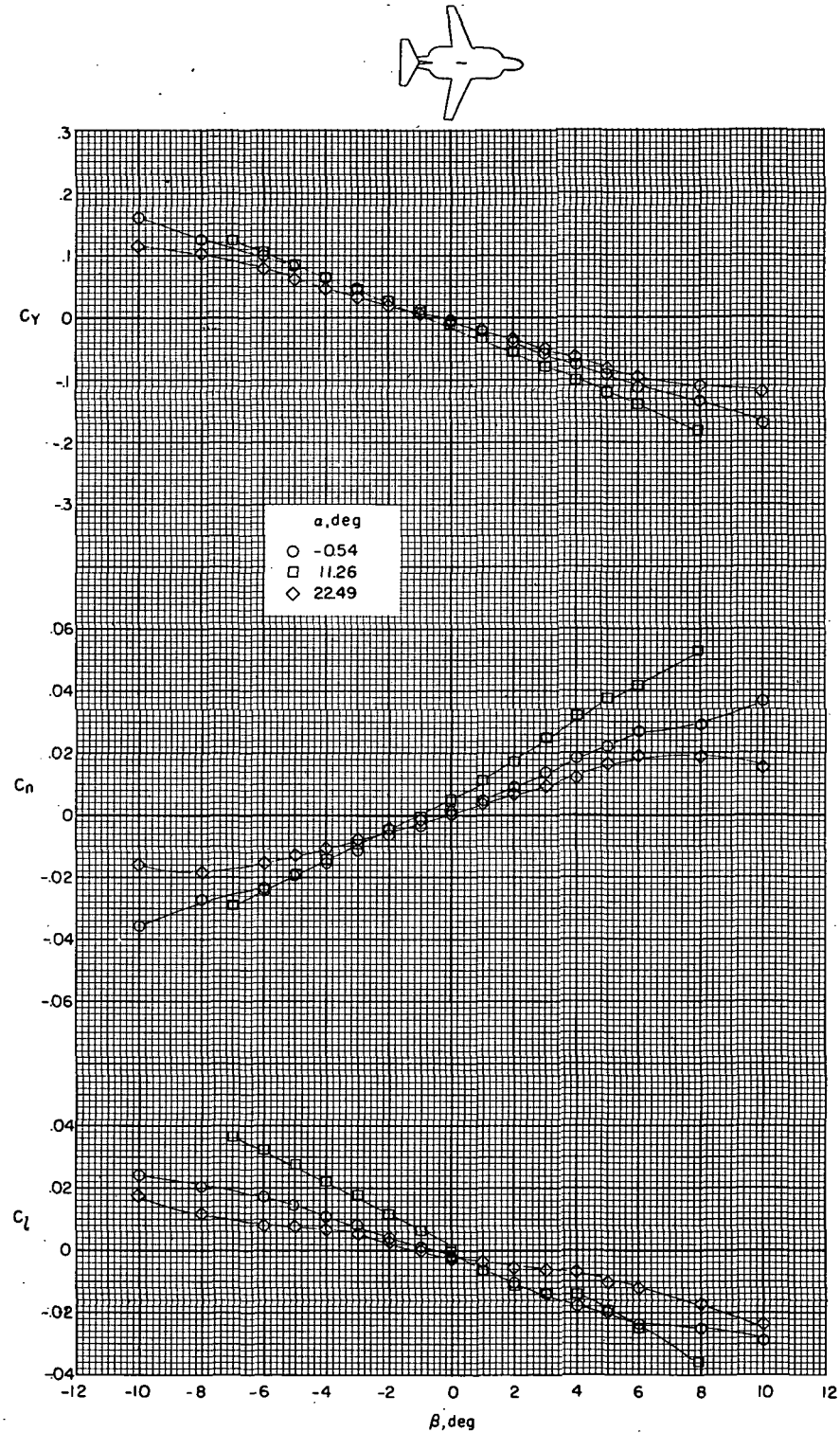

(b) Configuration 1, $i_t = 5^o$.

Figure 20.- Continued.

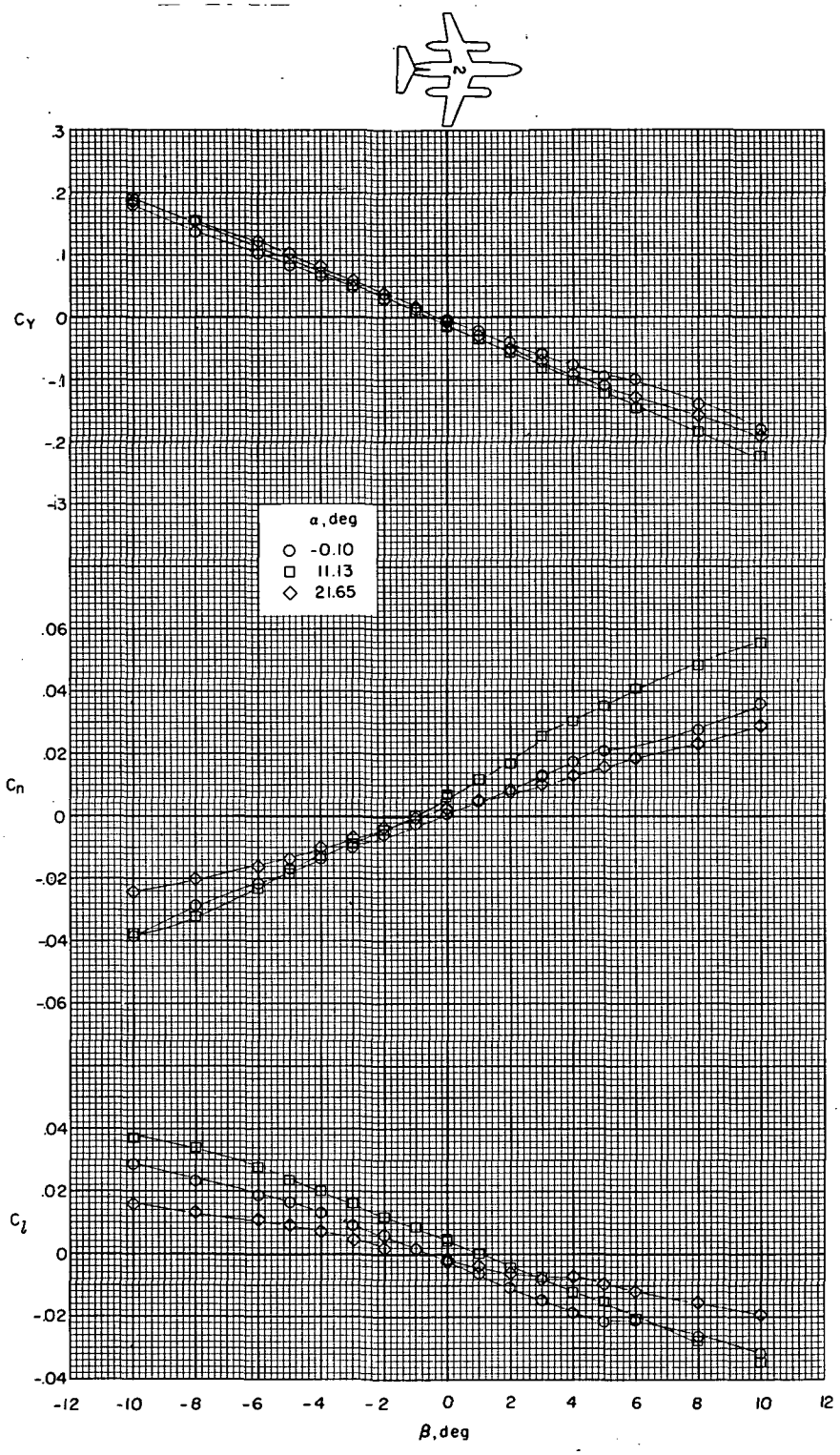

(c) Configuration 2, $i_t = 5^o$.

Figure 20.- Continued.

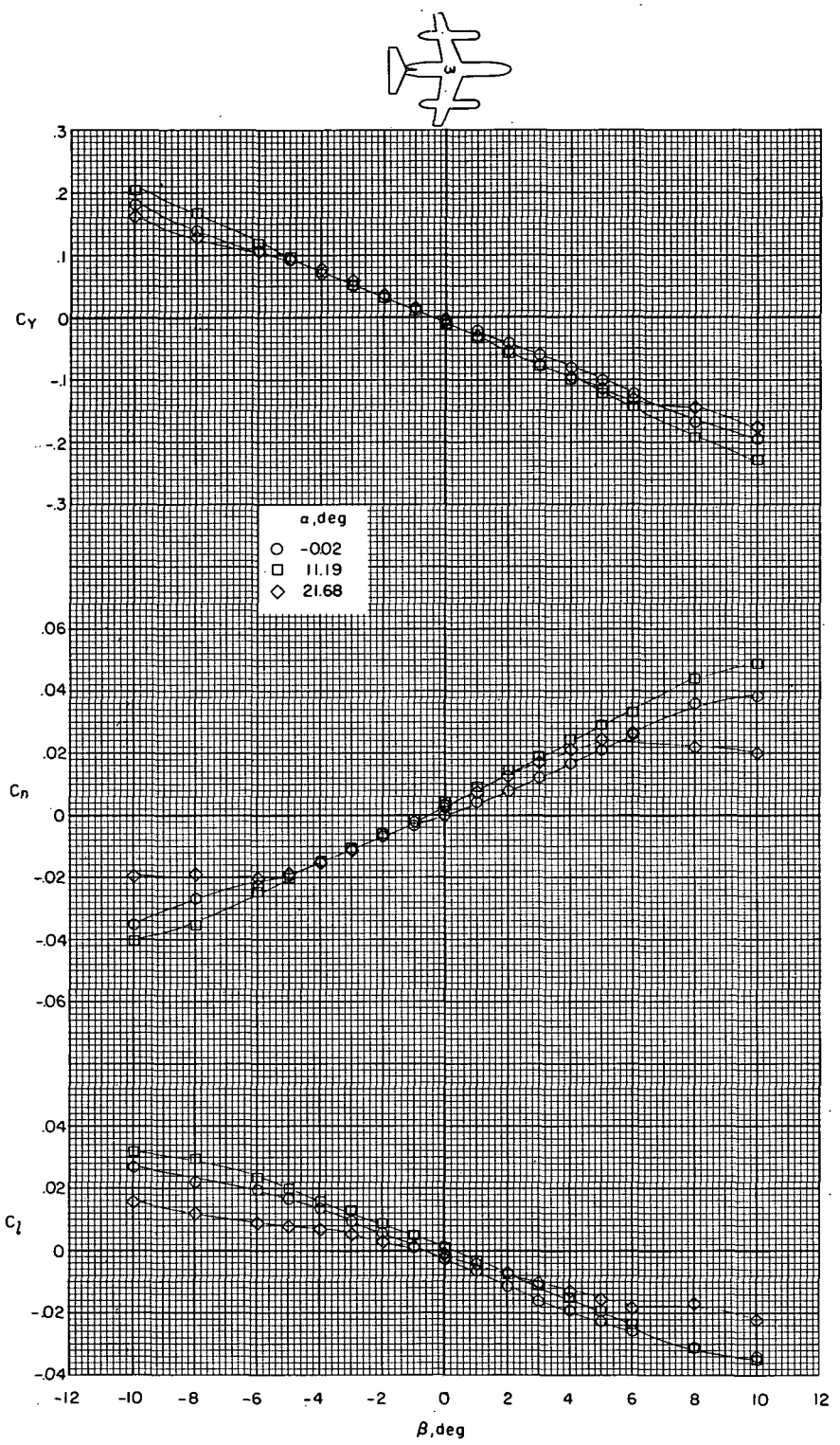

(d) Configuration 3, $i_t = 0^o$.

Figure 20.- Continued.

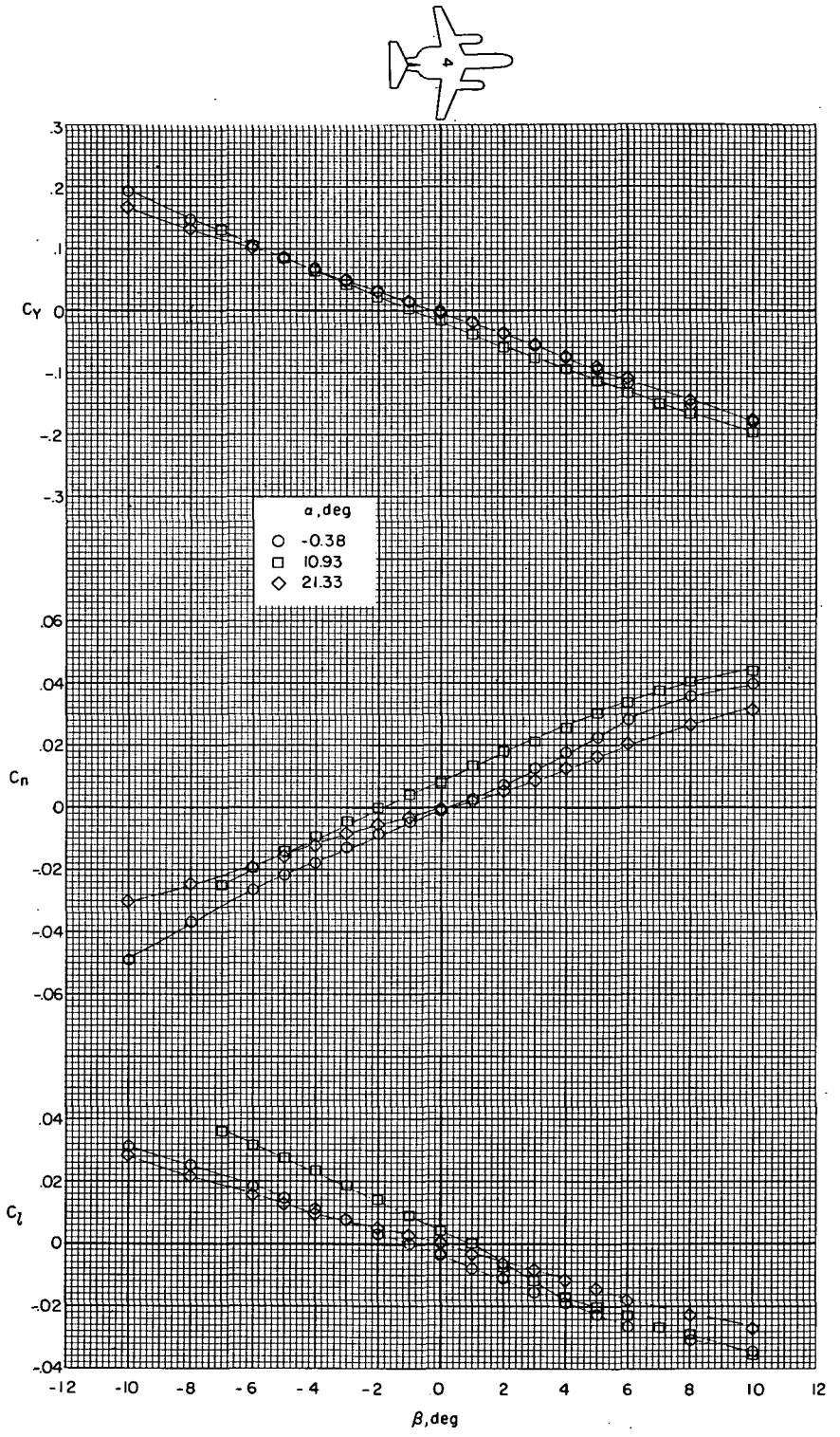

(e) Configuration 4, $i_t = 0^o$.

Figure 20.- Continued.

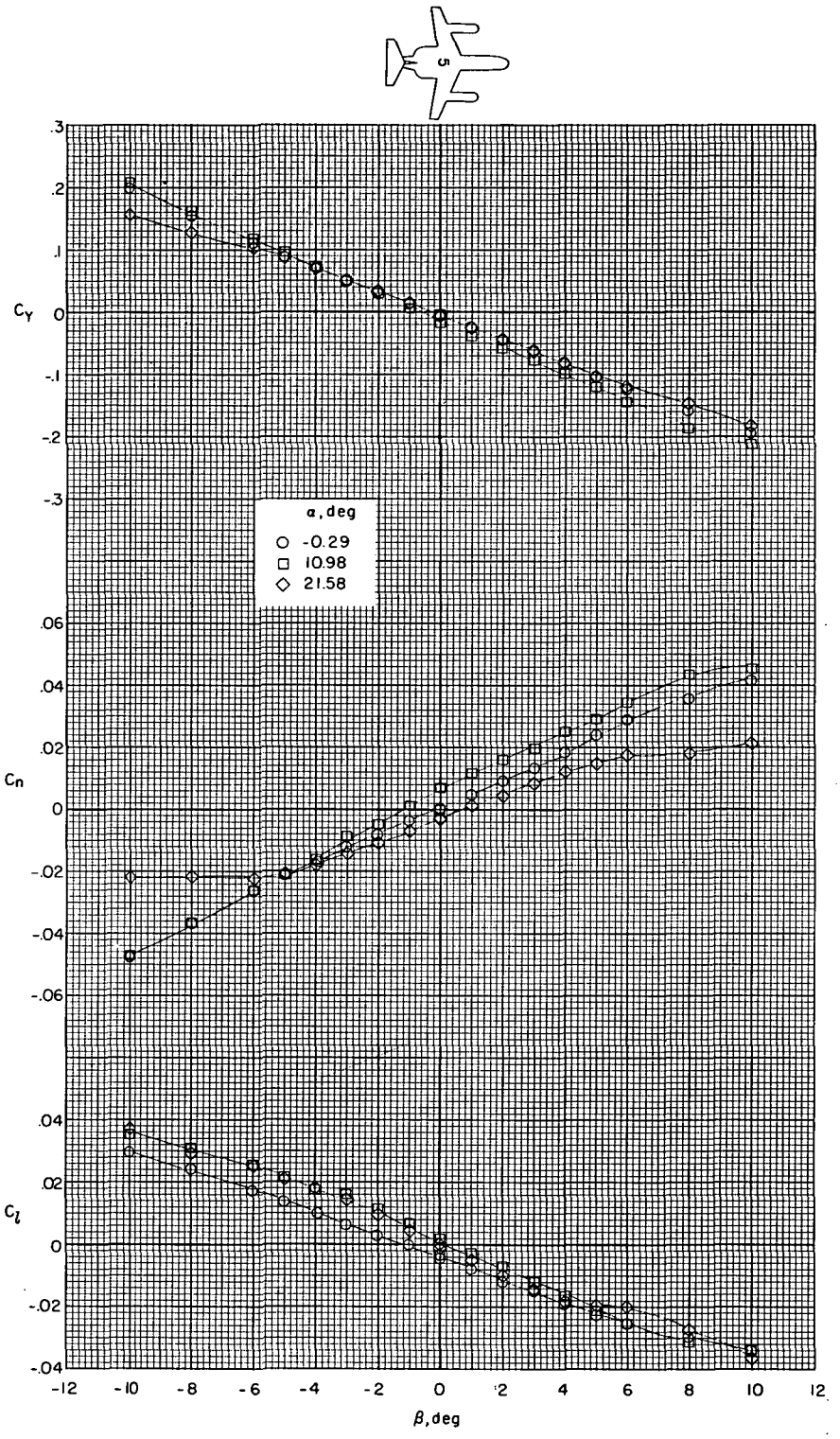

(f) Configuration 5, $i_t = 0^o$.

Figure 20.- Concluded.

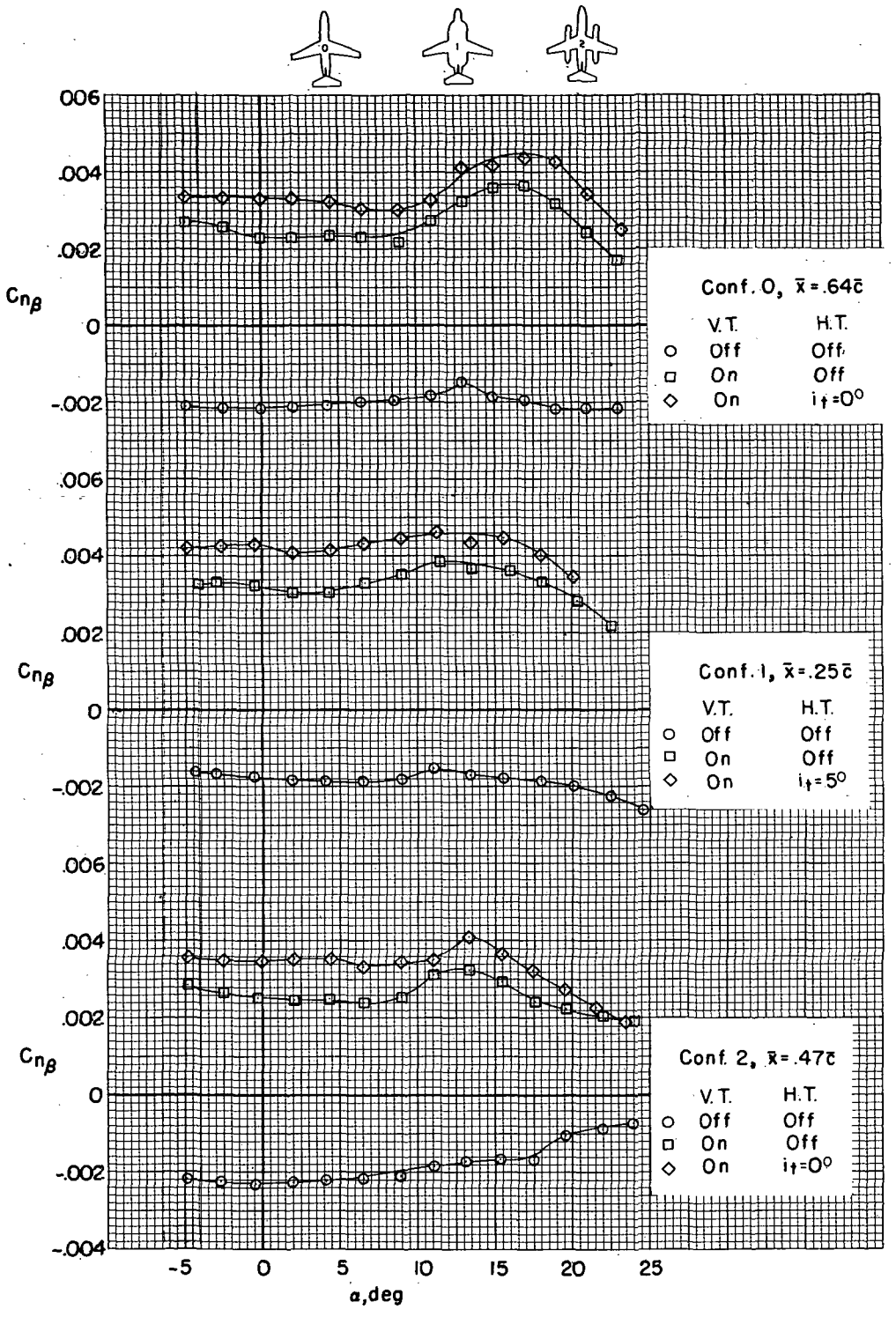

(a) Configurations 0, 1, and 2.

Figure 21.- Effect of empennage on directional-stability parameter with $\partial C_m/\partial C_L = -0.05$.

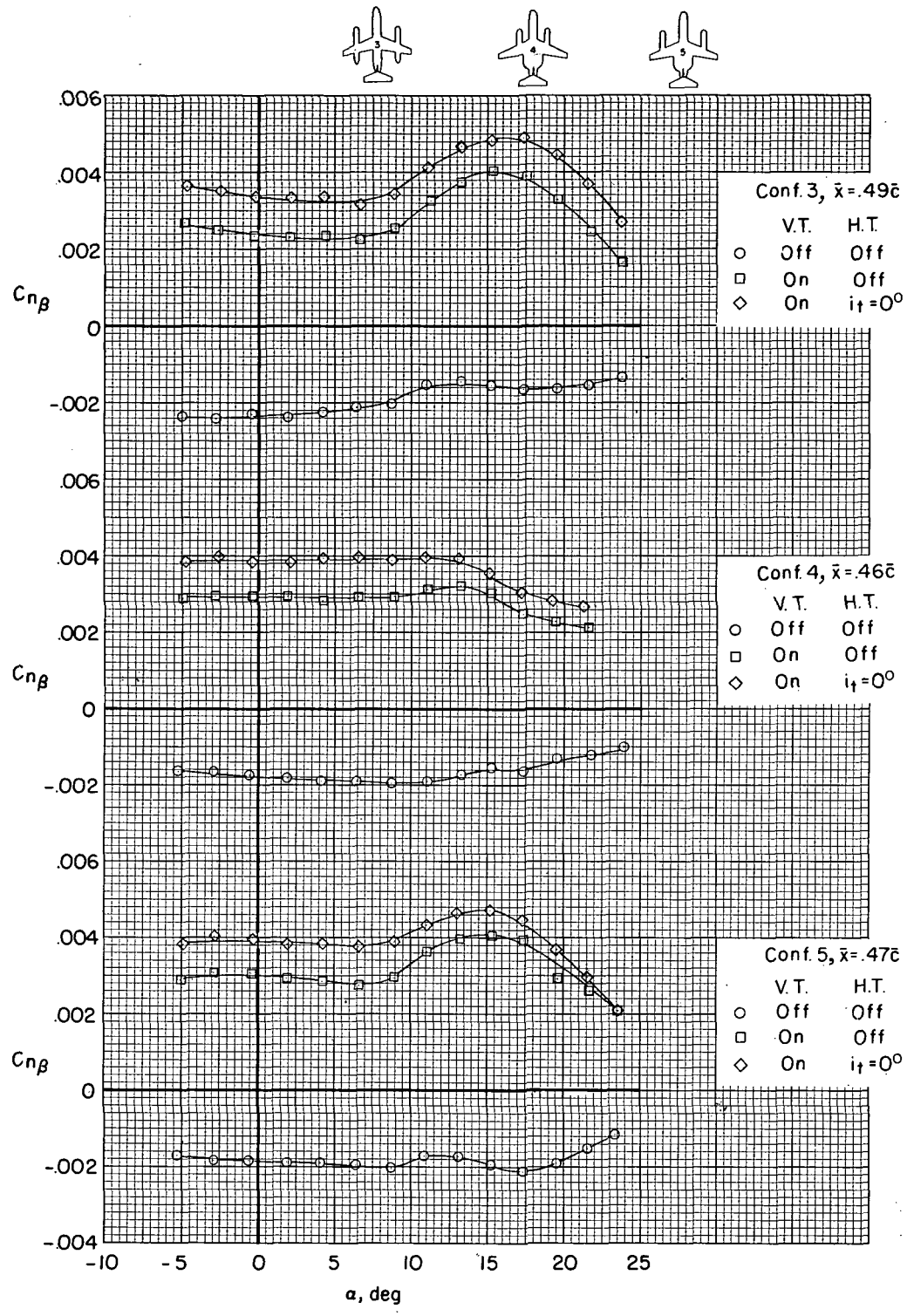

(b) Configurations 3, 4, and 5.

Figure 21.- Concluded.

NASA-Langley, 1973 — 1 L-8754

"The aeronautical and space activities of the United States shall be conducted so as to contribute . . . to the expansion of human knowledge of phenomena in the atmosphere and space. The Administration shall provide for the widest practicable and appropriate dissemination of information concerning its activities and the results thereof."

—NATIONAL AERONAUTICS AND SPACE ACT OF 1958

NASA SCIENTIFIC AND TECHNICAL PUBLICATIONS

TECHNICAL REPORTS: Scientific and technical information considered important, complete, and a lasting contribution to existing knowledge.

TECHNICAL NOTES: Information less broad in scope but nevertheless of importance as a contribution to existing knowledge.

TECHNICAL MEMORANDUMS: Information receiving limited distribution because of preliminary data, security classification, or other reasons. Also includes conference proceedings with either limited or unlimited distribution.

CONTRACTOR REPORTS: Scientific and technical information generated under a NASA contract or grant and considered an important contribution to existing knowledge.

TECHNICAL TRANSLATIONS: Information published in a foreign language considered to merit NASA distribution in English.

SPECIAL PUBLICATIONS: Information derived from or of value to NASA activities. Publications include final reports of major projects, monographs, data compilations, handbooks, sourcebooks, and special bibliographies.

TECHNOLOGY UTILIZATION PUBLICATIONS: Information on technology used by NASA that may be of particular interest in commercial and other non-aerospace applications. Publications include Tech Briefs, Technology Utilization Reports and Technology Surveys.

Details on the availability of these publications may be obtained from:

SCIENTIFIC AND TECHNICAL INFORMATION OFFICE

NATIONAL AERONAUTICS AND SPACE ADMINISTRATION

Washington, D.C. 20546